Pergamon

Geochimica et Cosmochimica Acta, Vol. 68, No. 13, pp. 2799–2814, 2004

0016-7037/04 $30.00 + .00

doi:10.1016/j.gca.2003.12.024

Biotransformation of two-line silica-ferrihydrite by a dissimilatory Fe(III)-reducing bacterium: Formation of carbonate green rust in the presence of phosphate

Ravi K. Kukkadapu,* John M. Zachara, James K. Fredrickson, and David W. Kennedy
Pacific Northwest National Laboratory, Richland, WA 99352, USA

(*Received November* 1, 2002; *accepted in revised form December* 22, 2003)

Abstract—The reductive biotransformation of two Si-ferrihydrite coprecipitates (1 and 5 mole % Si) by *Shewanella putrefaciens*, strain CN32, was investigated in 1,4-piperazinediethanesulfonic acid-buffered media (pH ~7) with lactate as the electron donor. Anthraquinone-2,6-disulfonate, an electron shuttle, was present in the media. Experiments were performed without and with PO_4^{3-} (P) (1 to 20 mmol/L) in media containing 50 mmol/L Fe. Our objectives were to define the combined effects of SiO_4^{4-} (Si) and P on the bioreducibility and biomineralization of ferrihydrites under anoxic conditions. Iron reduction was measured as a function of time, solids were characterized by powder X-ray diffraction and Mössbauer spectroscopy, and aqueous solutions were analyzed for Si, P, Cl^- and inorganic carbon. Both of the ferrihydrites were rapidly reduced regardless of the Si and P content. Si concentration had no effect on the reduction rate or mineralization products. Magnetite was formed in the absence of P whereas carbonate green rust GR(CO_3^{2-}) ($[Fe^{II}_{(6-x)}Fe^{III}_x(OH)_{12}]^{x+}(CO_3^{2-})_{0.5x} \cdot yH_2O$) and vivianite [$Fe_3(PO_4)_2 \cdot 8H_2O$], were formed when P was present. GR(CO_3^{2-}) dominated as a mineral product in samples with <4 mmol/L P. The Fe(II)/Fe(III) ratio of GR(CO_3^{2-}) varied with P concentration; the ratio was 2 in 1 mmol/L P and approached 1 with 4- and 10 mmol/L P. Green rust appeared to form by solid-state transformation of ferrihydrite. Media P and Si concentration dictated the mechanism of transformation. In the 1 mole % Si coprecipitate with 1 mmol/L P, an intermediate Fe(II)/Fe(III) phase with structural Fe(II) slowly transformed to GR with time. In contrast, when ferrihydrite contained more Si (5 mole %) and/or contained higher P (4 mmol/L), sorbed Fe(II) and residual ferrihydrite together transformed to GR. Despite similar chemistries, P was shown to have a profound effect on extent of ferrihydrite reduction and biotransformations while that of Si was minimal.

1. INTRODUCTION

Green rusts (GRs) are mixed valence, layered Fe(II)/Fe(III)-hydroxides that belong to the sjögrenite-pyroaurite mineral class (Taylor, 1973). These compounds have an ideal composition of $[Fe^{II}_{(6-x)}Fe^{III}_x(OH)_{12}]^{x+}[(A^{x/n})\cdot yH_2O]^{x-}$, where $A^{x/n}$ is an *n*-valent interlayer anion (e.g., Cl^-, CO_3^{2-}, PO_4^{3-}, SO_4^{2-}). They are found in hydromorphic soils and are potential contaminant reductants, anion exchangers, and metal cation sorbents in anoxic soils and sediments (Hansen et al., 1996; Myneni et al., 1997; Erbs et al., 1999; Lee et al., 2000; Loyaux-Lawniczak et al., 2000; Refait et al., 2000; Williams and Scherer, 2001; Bond and Fendorf, 2003). Recently, a bluish-gray colored GR mineral termed fougerite with Fe(II)/Fe(III) of ~1 was isolated from forest soils of Brittany (Trolard et al., 1997). Various synthetic procedures have been developed for GR that are believed to mimic those operative in the environment including: i) the controlled oxidation of ferrous hydroxide in the presence of Cl^-, SO_4^{2-}, and CO_3^{2-} (Génin et al., 1998), and ii) the solid-state transformation of ferrihydrite by $Fe^{2+}_{(aq)}$ (Mann et al., 1989; Hansen et al., 1994).

Dissimilatory Fe(III)-reducing bacteria (DIRB) catalyze the reduction of Fe(III) to Fe(II) in anoxic soils, sediments, and groundwater (Lovley and Phillips, 1986). A variety of biomineralization products result from the interaction of DIRB with poorly crystalline two-line ferrihydrite, including green rusts under specific conditions (Fredrickson et al., 1998). Fe(II) flux rate and magnitude at the ferrihydrite surface and the presence of sorbed/coprecipitated ions are important factors influencing the nature of the biomineralization products (Zachara et al., 2002). Medium composition and electron donor and acceptor concentrations are also important. In a 1,4-piperazinediethanesulfonic acid (PIPES)-buffered medium with 4 mmol/L P (a ligand with strong affinity for ferrihydrite surfaces) and 0.1 mmol/L anthraquinone-2,6-disulfonate (AQDS) (an electron shuttle), a carbonate GR [GR(CO_3^{2-}] in association with vivianite was the primary mineral product formed in an anoxic suspension with *S. putrefaciens* (CN32) (Fredrickson et al., 1998). A phosphate GR [GR(PO_4^{3-}], however, was identified as a major product of the bioreduction of ferrihydrite by *S. putrefaciens* in similar medium (with and without dissolved Ni^{2+}) but without AQDS (Parmar et al., 2001).

Although, GR has been observed as a product in the laboratory transformation of Fe(III) oxides by iron reducing bacteria, the specific range of chemical and biologic conditions that promote GR formation has not been established. Two out of three reports of biogenic GR formation (Fredrickson et al., 1998; Parmar et al., 2001) observed that P was requisite for its genesis. However, the specific mechanistic role of P in promoting GR formation is unknown. Under identical conditions, but in the absence of P, magnetite is the predominant bacterial transformation product of ferrihydrite (Fredrickson et al., 1998). Magnetite is thermodynamically more stable than GR (Génin et al., 1998), but P apparently impedes magnetite formation (Couling and Mann, 1985; Fredrickson et al., 1998). In contrast, GR was found as a primary anoxic transformation

* Author to whom correspondence should be addressed, at Pacific Northwest National Laboratory, P.O. Box 999, MSIN K8-96, Richland, WA 99352 (ravi.kukkadapu@pnl.gov).

product of lepidocrocite by *S. putrefaciens* strain CIP in the absence of P (Ona-Nguema et al., 2002). This latter study used a different buffer (bicarbonate), electron donor (formate), and higher organism concentrations (10x) than the former studies. Whether one of these factors or the organism itself was most influential in GR formation was not established. Lepidocrocite is the primary oxidation product of GR (Karim, 1986), implying structural or kinetic relationships between the two mineral phases. The only common requirement noted above in the biogenesis of GR from ferrihydrite appears to be the presence of excess electron donor.

Natural ferrihydrites contain Si (up to 9 mole %), and significant amounts of organic matter (Carlson and Schwertmann, 1981; Fox, 1989; Fortin et al., 1993; Tessier et al., 1996; Perret et al., 2000). Coreacted Si affects the recrystallization of ferrihydrite to crystalline oxides such as goethite and hematite and may influence its reductive transformation by DIRB. Silicate anions, like P, have a strong affinity for ferrihydrite (Carlson and Schwertmann, 1981; Cornell et al., 1987; Reeves and Mann, 1991; Zachara et al., 2002). A Si/Fe ratio of 0.005 strongly retarded the oxidative recrystallization of ferrihydrite at pH = 12, and promoted hematite formation over goethite (Cornell et al., 1987). Moreover, the extent of ferrihydrite conversion decreased with an increase in Si content, and Si concentration influenced the product morphology (Cornell and Giovanoli, 1987). Silica-ferrihydrite coprecipitates are more thermally stable towards transformation to hematite than pure ferrihydrites (Zhao et al., 1994).

The purpose of this study was to investigate the combined effect of Si and P on the biomineralization of ferrihydrite by *S. putrefaciens*, a facultative iron-reducing bacterium. Of particular interest were the effects of Si and P on GR and vivianite formation, and the role of other medium components in promoting the crystallization of one phase over the other. The influence of these anions on ferrihydrite biomineralization was explored by varying the Si-content of the ferrihydrite coprecipitates and the P content of the medium. Mineral products were analyzed as a function of incubation time using X-ray diffraction (XRD), Mössbauer spectroscopy, and electron microscopy. Insights are developed on the specific conditions required for the biogenesis of GR, and the factors controlling the Fe(II)/Fe(III) ratio of the biotransformation products.

2. MATERIALS AND METHODS

2.1. Materials

Two-line silica-ferrihydrite coprecipitates were prepared using ferric nitrate and sodium meta-silicate. The ferric nitrate was dissolved in deionized water, and the sodium meta-silicate was dissolved in anoxic, CO_2-free, 2 mol/L NaOH, both in Teflon bottles. Nitrogen gas was bubbled through the ferric nitrate solution for 30 min before gradually adding the silicate solution. After the silicate solution was added, the suspension pH was approximately 2.5. The pH of the suspension was increased by slow, sustained titration with anoxic, CO_2-free, 2 mol/L NaOH until the suspension pH was approximately 7.1. The pH-adjustment process took approximately 2 h. After overnight equilibration under an anoxic atmosphere, the suspension pH was 7.2. The mole percent of Fe and Si in solution before precipitation was 95 and 5%, or 98 and 2%, respectively, for two separate batches of Si-ferrihydrites. The Si-ferrihydrite precipitates were washed several times with anoxic, CO_2-free, 0.1 mol/L $NaClO_4$ to remove nitrate. The washed precipitates (in 0.1 mol/L $NaClO_4$) were stored under an anoxic atmosphere at room temperature (RT). A portion of the washed suspensions was dissolved in concentrated HCl and analyzed for Si and Fe by inductively coupled plasma-mass spectroscopy (ICP-MS, Hewlett Packard 4500). The ICP-determined Si/(Si + Fe) mole fractions of the two Si-ferrihydrites respectively were 0.013 and 0.048. These will be referred to as 0.01- and 0.05-Si-ferrihydrites.

2.2. Bacteria and Media

Anoxic suspensions of *S. putrefaciens* strain CN32 were prepared and suspended in a 30 mmol/L PIPES buffered-medium (pH ~7) as reported previously (Fredrickson et al., 2001). Media components included (in mmol/L): lactate, 27 (electron donor); AQDS, 0.09 (electron shuttle); NH_4Cl, 25.5; KCl, 1.2; $CaCl_2{\cdot}8H_2O$, 0.7; and varying amounts of phosphate (NaH_2PO_4), 0 or 1, 4, 10, and 20. The medium composition was similar to our previous study (Fredrickson et al., 1998) where biogenic GR was observed, except that the current media lacked trace minerals that included sulfate salts. Sulfate, a potential anion for GR, was excluded to prevent sulfate-GR formation.

Both 0.01- and 0.05-Si-ferrihydrites (~50 mmol/L Fe), which were "aged" for 1 and 3 months, were incubated in the PIPES buffered-media (30 mmol/L) containing $2–4 \times 10^8$ cells/mL. The headspace atmosphere of the tubes was O_2-free N_2. The tubes were sealed with butyl rubber stoppers. The tubes were incubated in the dark at 30°C and agitated (horizontally) at 100 rpm until sampled. Each treatment and sampling event was replicated three times, and separate tubes were sacrificed at each time-point for analyses. Abiotic control samples were setup at each time point. The control samples were devoid of cells, but were otherwise identical to the biotic samples.

2.3. Analyses

At selected time points, replicate tubes were removed from the incubator and transferred to an anaerobic (Ar:H_2, 95:5) glove bag (Coy Laboratory Products Inc., Grass Lake, MI). Four mL of suspension were transferred into a 10 mL plastic syringe fitted with a 0.2-μm filter unit. Approximately 0.5 mL of the filtrate (after discarding the first 20 drops of filtrate) were combined with 0.5 mL of anoxic 1 mol/L HCl in a polystyrene tube. This fraction was considered to be the aqueous or soluble fraction. Acid-extractable components were obtained by placing approximately 0.5 mL of suspension into a tube containing 0.5 mL 1 mol/L ultrex HCl and equilibrating for 24 h. This 0.5 N HCl extraction dissolved all the biogenic Fe(II). The equilibrated extracts were filtered with 0.2-μm polycarbonate syringe filters. The extracts and soluble fractions were analyzed for Fe(II), Fe_{total}, and Si. Phosphate and Cl^- were measured on aqueous samples. Inorganic carbon (IC) was measured on samples that showed appreciable biomineralization (Shimadzu TOC-5000A carbon analyzer). Fe(II) and Fe_{total} were measured using the ferrozine assay (Stookey, 1970). Fe_{total}, P, and Si concentrations were determined using an Agilent Technologies 4500 ICP/MS. Chloride was measured on a DX-500 Ion Chromatograph (Dionex Sunnyvale, CA) using an Ion Pac AS11 Anion Column (Dionex, Sunnyvale, CA). The pH, which varied between 7.4 and 8.1, was measured in the anaerobic glove bag with a Ross combination electrode.

2.4. Electron Microscopy and Powder X-ray Diffraction

Mineral residues were imaged with a LEO 982 FE SEM (field emission scanning electron microscope) operating at 3 kV fitted with backscatter and secondary electron detectors. The sample preparation was described previously (Zachara et al., 1998).

Powder XRD patterns were obtained with a Philips PW3040/00 X'Pert MPD system, using CuK_α radiation with a variable divergent slit and a solid-state detector. The routine power was 700 W (35 kV, 20 mA). Mineral suspensions were filtered through a 0.2-μm nylon filter and washed with 1 to 2 mL of acetone to obtain "dry" powder samples. The powders were tightly packed into the wells (1/4 inch diameter and 1/32 inch deep) of low-background quartz XRD slides (Gem Dugout Inc., Pittsburgh, Pennsylvania). Filtration, washing, and packing of the samples were carried out in an anoxic chamber whereas the XRD measurements were carried out at ambient atmosphere, 30 min scans (step size 0.04 °2θ/min). The JADE+, V5 (Materials Data Inc., Livermore, California) software package was used for data analysis.

2.5. ^{57}Fe Mössbauer Spectroscopy

Randomly oriented absorbers were prepared by mixing approximately 30 mg of "acetone-dried" sample with petroleum jelly in a 0.375 inch thick and 0.5 inch i.d. Cu holder sealed at one end with clear scotch tape. The holder was entirely filled with the sample mixture and sealed at the other end with scotch tape. An oxygen impermeable polymer film (aluminized Mylar) that was stable at 77 K was added as an outer seal on the both ends of the holder. Both the tape and polymer were snapped into the holder with rings made of carbonized-polyetheletherketone (PEEK) polymer to ensure tightness. The sample holders were stored in an anoxic chamber. Samples within the holders were stable towards oxidation. The Mössbauer spectra (77 K) of a "fresh" holder containing GR and the same holder left in an anoxic chamber for 15 d were identical.

Mössbauer spectra were collected using a 50 mCi (initial strength) ^{57}Co/Rh source. The velocity transducer MVT-1000 (WissEL) was operated in constant acceleration mode (23 Hz, ±10 mm/s or ±6 mm/s). An Ar-Kr proportional counter was used to detect the radiation transmitted through the holder, and the counts were stored in a multichannel scalar (MCS) as a function of energy (transducer velocity) using a 1024 channel analyzer. Data were folded to 512 channels to give a flat background and a zero-velocity position corresponding to the center shift (CS or δ) of a metallic iron foil at RT. Calibration spectra were obtained with a 20 μm thick α-Fe(m) foil (Amersham, England) placed in exactly the same position as the samples to minimize any errors due to changes in geometry. A top loading Janis exchange gas cryostat was used to cool the samples. For the 77 K measurements, both the source and drive assembly were held at RT.

All Mössbauer spectra were fitted with quadrupole splitting distributions (QSDs) and/or hyperfine splitting distributions (HFDs) using the Voigt-based fitting method of Rancourt and Ping (1991) and the Recoil program (University of Ottawa, Canada). In the Voigt-based method, each distribution (QSD/HFD) is represented by a sum of Gaussians having different positions, widths and relative areas. A minimum number of Gaussians was used to obtain a good statistical fit. Sample thickness corrections were not carried out. Spectral areas, reported as percent of total, were computed for each of the contributing sites. Statistics were computed for these spectral areas that were dependent on the number of data points (that were the same for each sample), the number of Fe sites, and the number of parameters describing each site. The coefficients of variation of the spectral areas of the individual sites generally ranged between 2 and 5% of the fitted value. The spectral areas were equated with the mass percentage of the different sites given the assumption of a constant recoil factor. The following general guidelines were used in the modeling of the Mössbauer data: 1) the Lorentzian half width at half maximum (HWHM) was fixed at the minimum line width (0.097 mm/s) of the ^{57}Fe 14.4 keV Mössbauer transition, 2) all doublets were assumed symmetric, 3) the ratios of the spectral areas of peak 1 to peak 3, and peak 2 to peak 3 of the sextets were fixed at 3 and 2, respectively, and 4) no coupling was allowed between δ or center shift (CS), with the distributed hyperfine parameter (Δ or QS or quadrupole shift), or between ε (quadrupole shift parameter) and the distributed hyperfine parameter (z).

3. RESULTS

3.1. Aqueous Chemistry

Aqueous concentrations of Fe(II), Fe_{total}, Si, P, Cl^-, and inorganic carbon (IC) of both the control and the bioreduced samples were measured to follow the distribution of these ions between the solution and solid phase. Inorganic C was generated by the bacterial oxidation of lactate (Fredrickson et al., 1998), and its presence was an indication of liberated electron equivalents.

3.1.1. Si

Significant concentrations of aqueous Si were released from the coprecipitates in the control suspensions (Figs. 1a,b). A higher percentage of the coprecipitated Si was released by the 0.01-Si-ferrihydrite (20 to 80% of the total). For example, in <4 mmol/L P samples, <0.4 and ~2 mmol/L Si was retained respectively by 0.01-and 0.05-Si-ferrihydrites. The aqueous Si concentration tended to increase with an increase in P concentration, suggesting surface or structural anion exchange. Others have found that P is capable of displacing sorbed Si in ferrihydrite (Vempati and Loeppert, 1989; Parfitt et al., 1992). Si was more strongly retained by the 0.05-Si-ferrihydrite for unknown reasons.

The dissolved Si concentrations in the ferrihydrite suspensions incubated with CN32 were similar to their respective controls when p <4 mmol/L (Figs. 1c,d). At 10- and 20-mmol/L P, however, aqueous Si concentrations were significantly lower than controls. For example, dissolved Si in the 0.01-Si-ferrihydrite system was ~20% in the bioreduced suspension as compared to ~80% in the control when P was 20 mmol/L. The decrease in Si concentration at higher P concentrations may be due to incorporation into mineral transformation products of ferrihydrite.

3.1.2. Phosphate

Both of the Si-ferrihydrites (controls) exhibited strong affinity towards P (data not shown). Almost all of the 1- and 4-mmol/L P was adsorbed by ferrihydrite. The higher P concentrations (≥10 mmol/L) saturated the ferrihydrite surface. Aqueous P concentrations in the 10 and 20 mmol/L P media were approximately 3 and 12 mmol/L, respectively. The adsorption maxima of the Si-ferrihydrites for P ranged between 1.9 to 2.5 mmol/g of ferrihydrite. Phosphate sorption was generally higher in the 0.05-Si-system, and in the 8 d control samples. The observed adsorption maxima were higher than those reported for an air-dried pure ferrihydrite (0.6 and 1.3 mmol/g, Ryden et al., 1977). In contrast, P concentrations were below the ICP detection limit (<0.2 mg/L) in all the bioreduced samples, regardless of the initial P concentration or the Si content of the ferrihydrite. All of the P was incorporated into the residual ferrihydrite or its biotransformation products.

3.1.3. Inorganic carbon and chloride

Dissolved inorganic carbon (IC) was measured in the 0.01-Si-ferrihydrite suspension that was incubated with CN32 for 28 d. The observed aqueous concentrations of IC were compared to a theoretical total IC value that was calculated from published values of Fe(II) yield from bacterial lactate oxidation to CO_2 and acetate [1 HCO_3^- anion produced/4 Fe(II); Fredrickson et al., 1998]. The difference between the calculated total IC and the aqueous IC was considered to be sorbed or precipitated IC. The sorbed IC concentration of the bioreduced mineral fraction decreased with an increase in the P concentration of the medium (Fig. 2).

The aqueous Cl^- concentration was measured to determine if GR(Cl^-) was a possible product of ferrihydrite bioreduction. The measured Cl^- in the aqueous phases of all the bioreduced samples was virtually identical to that of their corresponding controls, indicating little or no discernable incorporation into mineral transformation products.

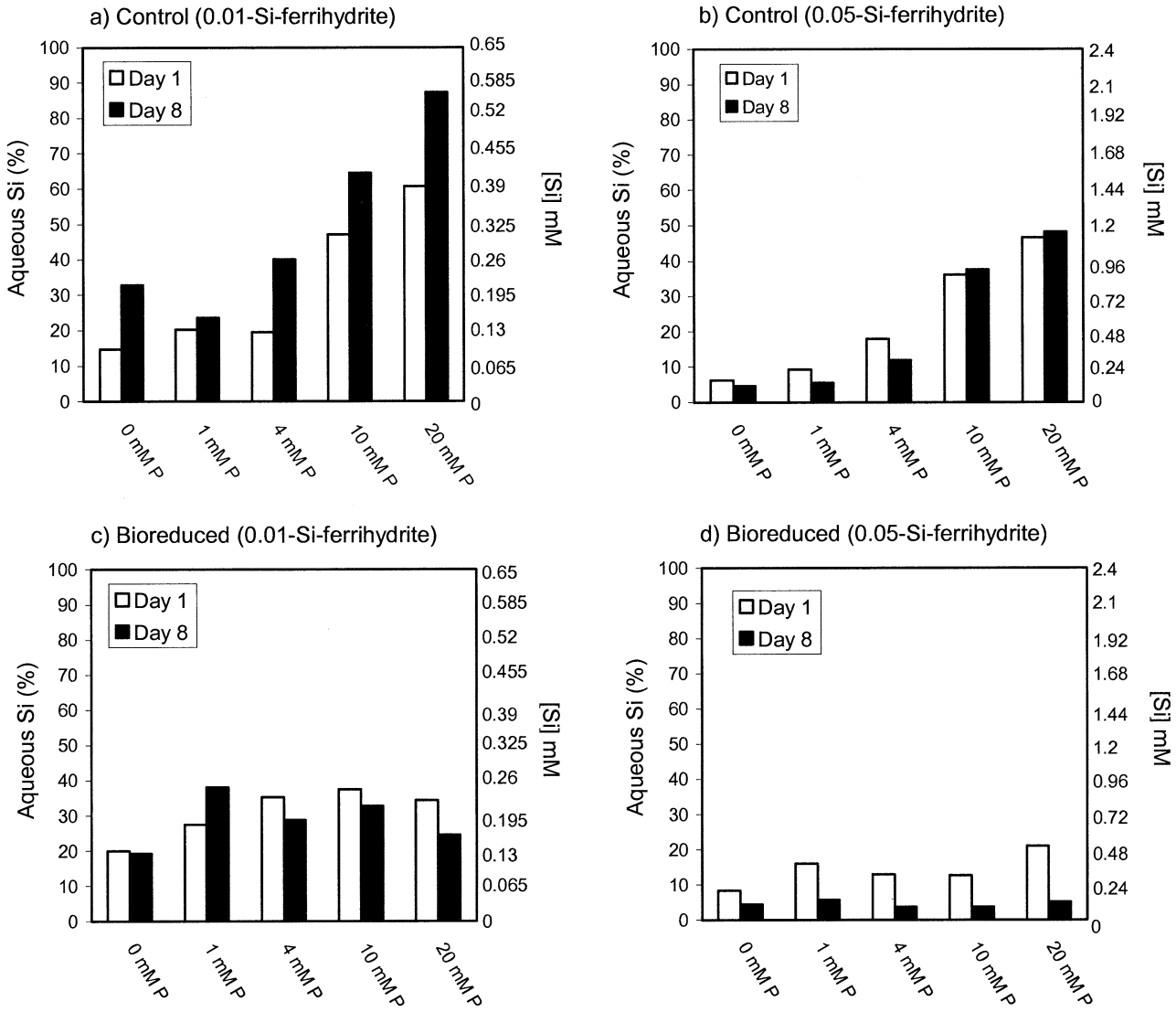

Fig. 1. Aqueous Si concentrations in control (a, b) and in incubated (c, d) Si-ferrihydrite suspensions. Note that the left-hand axis is the percent of total Si that was released to the aqueous phase. The right-hand axis is aqueous Si in mmol/L.

3.2. Reduction extent

The amount of Fe(II) production, and the distribution of Fe(II) between the aqueous and solid phase, was similar for the two Si-ferrihydrites when incubated with CN32 (Fig. 3). Increasing P promoted higher levels of Fe(II) production, but decreased aqueous phase concentrations of Fe^{2+}. Data for the control samples [$Fe(II)_{total}$, $Fe^{2+}{}_{(aq)}$] were not shown in Figure 3 because they were <0.5% of the inoculated samples. Greater than 90% of the Fe(III) present as ferrihydrite was reduced in the presence of 20 mmol/L P. The reduction process mediated by CN32 was rapid, and was approximately 65% complete within 1 d of inoculation (Fig. 3). Additional reduction occurred between day 1 and 8, with the amount being greater with 0.05-Si-ferrihydrite. Longer incubation periods (28 d and 15 months for 1 mmol/L P treatment with 0.01-Si-ferrihydrite) resulted in no additional reduction in spite of significant residual Fe(III) and lactate. Aqueous Fe^{2+} concentrations were well

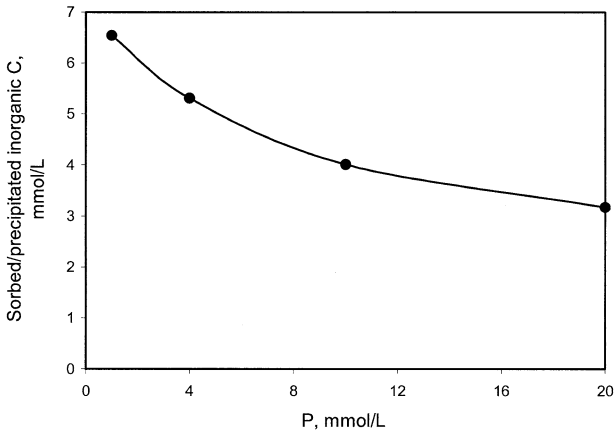

Fig. 2. Influence of media P concentration on sorbed/precipitated inorganic C. Data points are connected by line to discriminate different times and conditions.

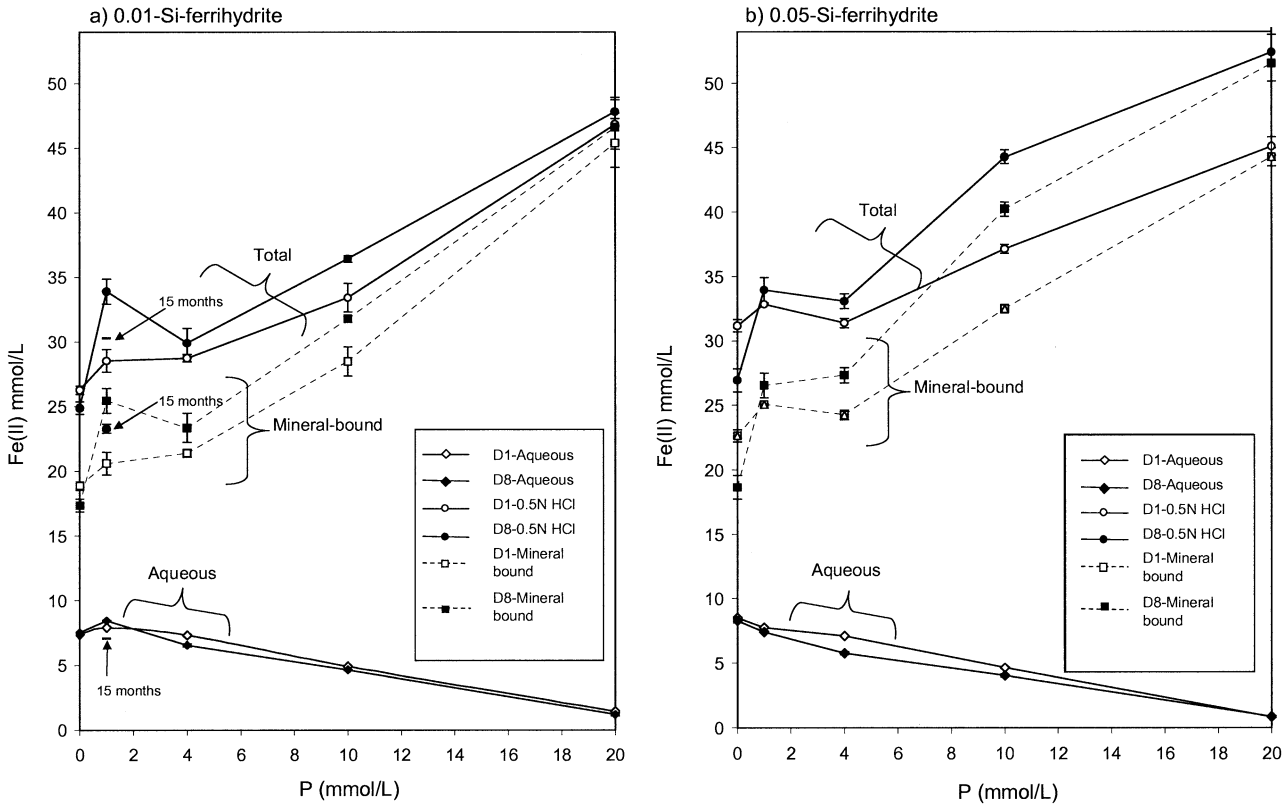

Fig. 3. Extractable Fe(II) (0.5 N HCl), aqueous and mineral-bound Fe^{2+} contents as a function of the P content of the media: (a) 0.01-Si-ferrihydrite and (b) 0.05-Si-ferrihydrite. Data points are connected as a guide to the eye.

below $Fe(II)_{total}$ for both ferrihydrites, indicating that most of the biogenic Fe(II) was mineral bound and/or precipitated in the residue.

3.3. X-ray Diffraction

Freshly synthesized 0.01- and 0.05-Si-ferrihydrite coprecipitates exhibited similar XRD spectra (Fig. 4; shown for 0.01-Si-ferrihydrite only). Prolonged aging (e.g., 8 months) in the media had a negligible effect on their XRD features. Such stability was expected because Si and P retard ferrihydrite crystallization (Kandori et al., 1992; Cornell and Schwertmann, 1996). Two broad peaks dominated the XRD spectrum of the Si-ferrihydrites. Their spectra were different from that of typical two-line ferrihydrite in the relative intensities of the two peaks (Parfitt et al., 1992; Zhao et al., 1994; Rancourt et al., 2001). In typical two-line ferrihydrite, the first peak at 0.25 nm (35° 2θ) is generally more intense than the peak at 0.15 nm (62° 2θ). A decrease in the ratio of the 0.25- to 0.15-nm peaks in arsenate-ferrihydrite coprecipitates was interpreted to result from Fe-O-As coordination on the ferrihydrite surface (Waychunas et al., 1996; Rancourt et al., 2001). The XRD spectrum in Figure 4, by analogy, indicated appreciable Fe-O-Si linkages on the ferrihydrite surface.

3.3.1. The 1 d bioreduced samples

Significant mineralogic changes occurred to the Si-ferrihydrites after 1 d of incubation with CN32, except in the media with 4 mmol/L P (Figs. 5a,c). The extent of Si substitution had no discernable effect on the identity of the biotransformation products. The media concentration of P

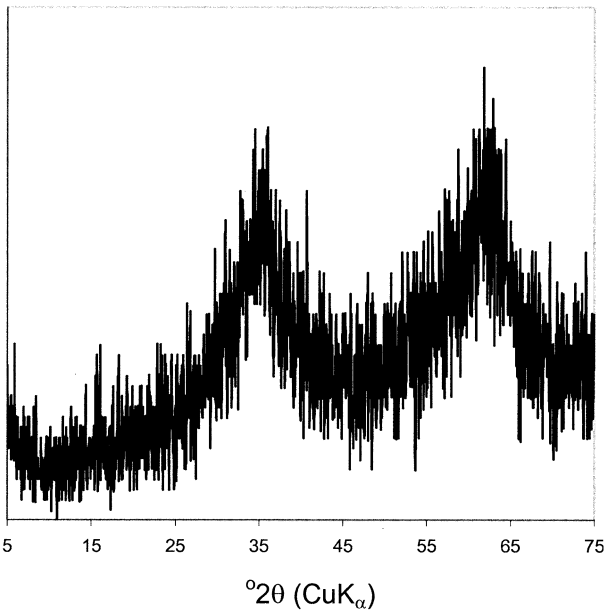

Fig. 4. Powder XRD spectrum of 0.01-Si-ferrihydrite in 1 mmol/L P medium.

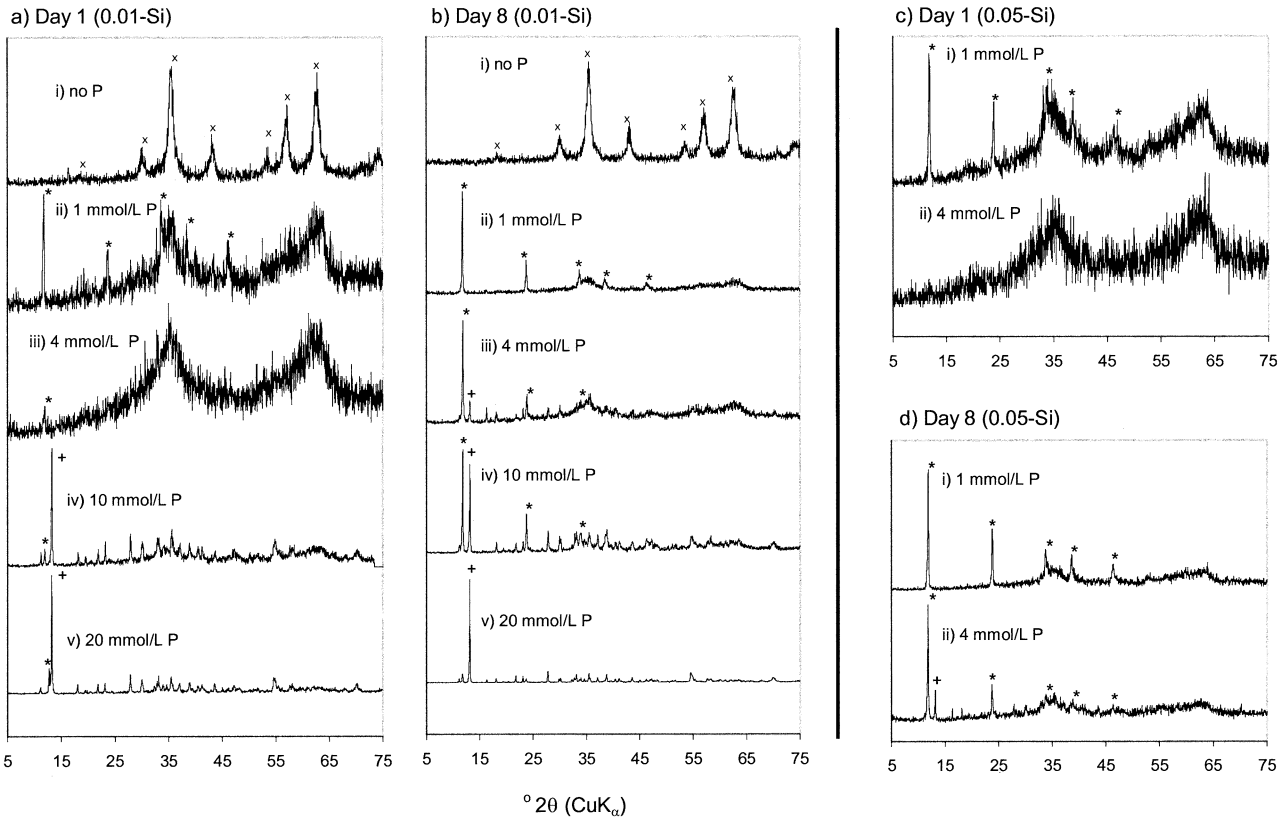

Fig. 5. Powder XRD spectra of Si-ferrihydrites that were incubated with CN32 and various media concentrations of P. (a, b) 0.01-Si-ferrihydrite after day 1 and day 8, and (c, d) 0.05-Si-ferrihydrite after day 1 and day 8. Magnetite, green rust, and vivianite peaks are indicated respectively by x, *, and +.

(Fig. 3a) had a major impact on the nature and extent of biomineralization.

X-ray diffraction peaks with *d*-spacings of fine-grained magnetite were observed in the absence of P (Fig. 5a-i). The extent of Fe(III) reduction in this sample (Fig. 3a), was consistent with complete conversion of ferrihydrite to magnetite where approximately 66% of the total Fe is in ferric form [$Fe(II)Fe(III)_2O_4$]. Magnetite was the primary transformation product observed after the bioreduction of two-line ferrihydrite and Ni-substituted ferrihydrite by CN32 (Fredrickson et al., 1998, 2001).

A combination of green rust (d_{003} 0.75 nm, 11.9° 2θ) and ferrihydrite was observed in the mineral residue of 0.01- and 0.05-Si-ferrihydrites incubated with 1 mmol/L P (Figs. 5a-ii and 5c-i). The peak at 0.75 nm (11.9° 2θ) was characteristic of green rust one (GR1) compounds that incorporate planar anions (e.g., CO_3^{2-}, Cl^-) in their interlayers (Bernal et al., 1959). In contrast, green rust two compounds (GR2) intercalate tetrahedral anions (PO_4^{3-}, SO_4^{2-}) for charge compensation. Phosphate GR exhibits a sharp peak (d_{003}) at 1.09 nm (8.14° 2θ) (Hansen and Poulsen, 1999) that was not observed here. X-ray diffraction analysis alone could not identify whether our biogenic GR1 was of the CO_3^{2-} or Cl^- form since both exhibit similar *d*-spacings. However, an absence of Cl^- removal from the media and the observed incorporation of significant carbonate (Fig. 2) in the mineral residue with 1 mmol/L P indicated the formation of GR(CO_3^{2-}).

The mineral residues from the 4 mmol/L P media showed little evidence for transformation to new crystalline phases after 1 d of incubation (Figs. 5a-iii and 5c-ii). The most intense diffraction line of GR was barely evident in the 0.01-Si-ferrihydrite mineral residue. The Si-ferrihydrites incubated with the highest concentrations of P (10 and 20 mmol/L) were transformed primarily to vivianite [$(Fe_3(PO_4)_2 \cdot 8H_2O$; 0.67 nm (13.2° 2$\theta$); Figs. 5a-iv,v]. Small amounts of green rust were also present with both P concentrations, and some residual ferrihydrite was evident at 10 mmol/L P (Figs. 5a,iv).

3.3.2. *The 8 d bioreduced samples*

The XRD patterns for the 0.01- and 0.05-Si-ferrihydrites that were incubated for 8 d showed evolution and change from the day 1 samples that were consistent with the Fe(II) concentrations in Figure 3. The 0.01- and 0.05-Si-ferrihydrite suspensions again exhibited comparable diffraction patterns after 8 d. The most dramatic changes between day 1 and day 8 were observed for the 1 and 4 mmol/L P treatments (Figs. 5b,d). Mineral residues from the 1 and 4 mmol/L P incubations showed significant crystallization to GR (Figs. 5b-ii,iii and 5d). GR formed in 10 mmol/L P media at the apparent expense of vivianite (compare 5a-iv with 5b-iv). Green rust was the prominent transformation product at low and intermediate P concentrations, while vivianite dominated at higher P.

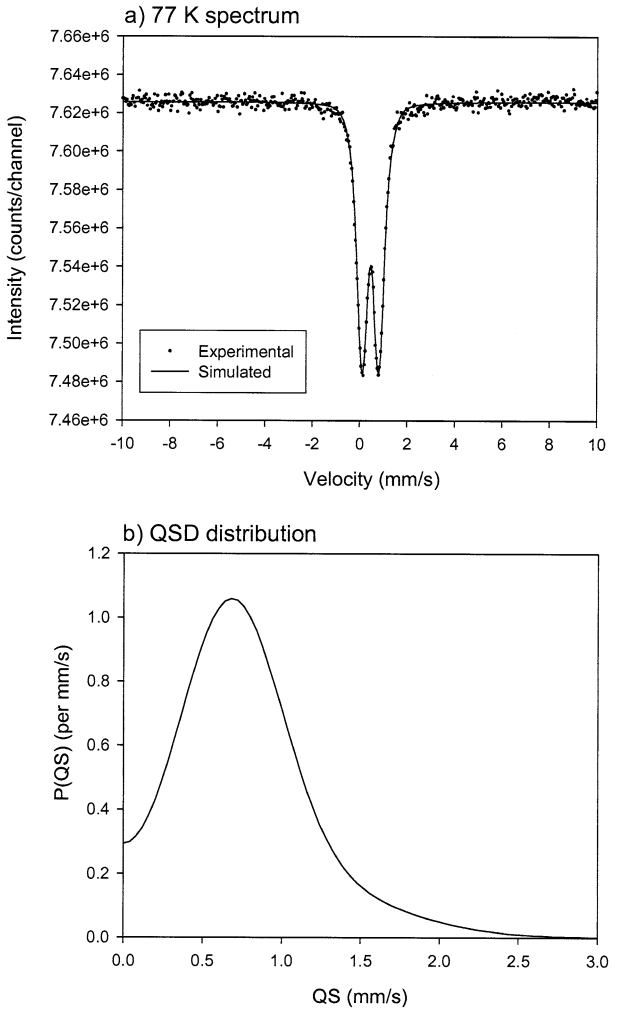

Fig. 6. The 77 K Mössbauer spectra of 0.01-Si-ferrihydrite in 1 mmol/L P medium. (a) Mössbauer spectrum with modeling based on the QSD method of Rancourt and Ping (1991) (also in Figs. 7–10) and (b) QSD two-component distribution.

3.4. Mössbauer spectroscopy

Both the "fresh" (as synthesized) and control Si-ferrihydrites, regardless of equilibration time and P concentration, exhibited identical RT and 77 K spectra. The 77 K spectrum of 1 mmol/L P, 0.01-Si-ferrihydrite (Fig. 6) displayed a doublet with the following derived Mössbauer parameters: δ (average center shift) = 0.46 mm/s, Δ (average quadrupole splitting) = 0.83 mm/s, and σ_{QSD} (standard deviation of QSD) = 0.52 mm/s. The Mössbauer parameters for the Si-ferrihydrites were similar to those reported for synthetic Ni-ferrihydrite (4 mole % Ni) (Kukkadapu et al., 2003), which was also fitted with the distribution method of Rancourt and Ping (1991). The RT spectra of all our Si-ferrihydrites (not shown) were also identical to those of naturally occurring Si-containing ferrihydrites (Murad and Schwertmann, 1988).

Room temperature and liquid nitrogen Mössbauer measurements were performed on select bioreduced mineral residues (1- and 4-mmol/L P, 0.01- and 0.05-Si-ferrihydrites; and 10 and 20 mmol/L P 0.01-Si-ferrihydrite) to provide insights on GR formation, Fe(II)/Fe(III) valence distribution, and the relative concentration of the different biotransformation products. The derived Mössbauer parameters of the samples are summarized in Table 1.

Table 1. The 77 K Mössbauer parameters.[a]

P, mmol/L	Fe-mineral	<CS> (mm/s)	<QS> (mm/s)
	0.01-Si-Ferrihydrite		
1 (day 1)[b]	Fe(II) (GR + GR*)	1.21	2.09
	GR Fe(III) + GR* Fe(III) + *spm* (II) & Fe(III)]	0.35	0.78
1 (day 1)	Fe(II) (GR + GR*)	1.26	2.82
	Fe(III) (GR + GR*)	0.47	0.46
	spm [Fe(II) + Fe(III)]	0.83	—
1 (day 8)	Fe(II) (GR + GR*)	1.26	2.83
	Fe(III) (GR + GR*)	0.47	0.43
	spm [Fe(II) + Fe(III)]	0.94	—
1 (15 months)	Fe(II) (GR)	1.27	2.88
	Fe(III) (GR)	0.47	0.44
4 (day 1)[b]	Fe(II) (GR + GR*)	1.2	2.1
	Fe(III) (GR + GR* + RF)	0.37	0.79
4 (day 1)	Fe(II) (GR + GR* + Sorb)	1.25	2.71
	Fe(III) (GR + GR* + RF)	0.47	0.70
4 (day 8)	Fe(II) (GR)	1.28	2.84
	Fe(III) (GR + RF)	0.50	0.87
	Vivianite-Fe1	1.32	2.56
	Vivianite-Fe2	1.34	3.24
	Unidentified	1.23	2.15
10 (day 8)	Fe(II) (GR)	1.21	2.83
	Fe(III) (GR + RF)	0.48	0.44
	Vivianite-Fe1	1.38	2.70
	Vivianite-Fe2	1.37	3.14
20 (day 8)	Fe(II) (GR)	1.11	2.69
	Fe(III) (GR + RF)	0.52	0.61
	Vivianite-Fe1	1.33	2.55
	Vivianite-Fe2	1.34	3.14
	0.05-Si-Ferrihydrite		
1 (day 1)[b]	Fe(II) (GR + GR*)	1.16	1.90
	Fe(III) (GR + GR* + RF)	0.33	0.62
1 (day 1)	Fe(II) (GR + GR*)	1.26	2.62
	Fe(III) (GR + GR* + RF)	0.48	0.92
4 (day 1)[b]	Fe(II) (GR*)	1.19	2.08
	Fe(III) (GR* + RF)	0.36	0.80
4 (day 1)	Fe(II) (GR* + Sorb)	1.26	2.63
	Fe(III) (GR* + RF)	0.47	1.05

[a] <CS> = average center shift; <QS> = average quadrupole shift; GR = green rust; GR* = green rust-like; Sorb = sorbed; *spm* = superparamagnetic; RF = residual ferrihydrite.
[b] RT Mössbauer spectra.

In addition to the ferrihydrite, GR and vivianite evident by XRD, other Fe species were tentatively identified in the bioreduced mineral residues by Mössbauer spectroscopy. These included: i) a GR-like phase [GR*], ii) sorbed Fe(II), and iii) a mixed Fe(II) and Fe(III) superparamagnetic (*spm*) phase [Fe(II)/Fe(III) *spm*]. These transitory Fe(II) containing species were identified by their Mössbauer response and apparent lability towards oxygen during the XRD analyses. GR* exhibited Mössbauer parameters similar to GR at RT and 77 K, but unlike GR, GR* rapidly oxidized to ferrihydrite during XRD analysis. Unlike GR*, dried GR powders are relatively stable towards oxidation (Williams and Scherer, 2001). Sorbed Fe(II) differed from GR and GR* in that it was "invisible" in the RT Mössbauer spectra and appeared as a doublet at 77 K. Sorbed Fe(II)

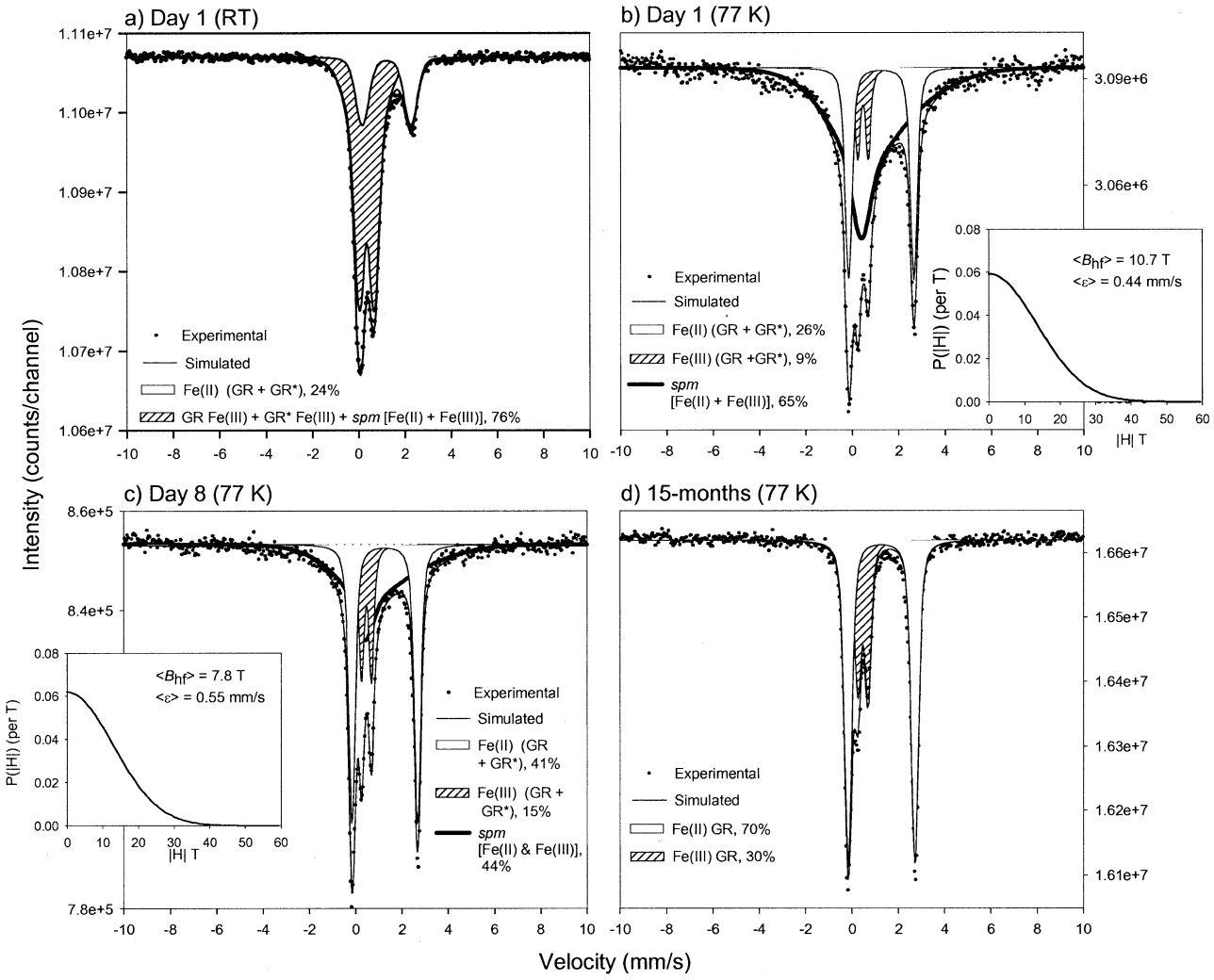

Fig. 7. Mössbauer spectra of 0.01-Si-ferrihydrite/1 mmol/L P after various incubation periods. (a, b) RT and 77 K Mössbauer spectra of the day 1 mineral residue. (c, d) The 77 K Mössbauer spectra of 8 d and 15 month samples showing the effect of time on transformation of GR* and *spm* phases to GR with time. HFD distributions of *spm* phase are shown as inserts (c, d).

may exist in an adsorbed state or as poorly crystalline, poorly defined precipitate. Adsorbed Fe(II) on layer silicates is "invisible" at RT due to a low recoil-fraction (Diamant and Pasternak, 1982). Sorbed Fe(II) also oxidized rapidly to ferrihydrite when contacted with atmosphere. The mixed superparamagnetic Fe(II)/Fe(III) phase existed in our Mössbauer spectra as doublet at RT and as collapsed sextet at 77 K.

The following guidelines were employed in modeling the Mössbauer spectra. First, the Fe(II) doublet feature in all the bioreduced residues, regardless of whether it was a unique Fe(II) site [GR, GR* or sorbed Fe(II)] or a site mixture, was fitted with only one doublet. A two component gaussian QSD distribution was used to model mixtures of Fe(II) sites when required. This approach was taken because it was not possible to uniquely discriminate the precise contributions of individual Fe(II) sites in mixtures. Second, the concentration ratio of the two octahedral Fe(II) sites of vivianite (Fe1 and Fe2) were fixed at a 1:2 ratio, in accordance with its crystal structure (Gonser and Grant, 1967). The plausibility that oxidized vivianite (Rouzies and Millet, 1993) and/or Si substituted vivianite could form in this system was given due consideration. Third, the central Fe(III) doublet of the 4-, 10-, and 20-mmol/L P, day 8 bioreduced samples, that was a mixture of Fe(III) from GR and residual ferrihydrite, was fitted with one Fe(III) doublet containing two components.

3.4.1. *The 0.01-Si-ferrihydrite with 1 mmol/L P*

Doublets due to Fe(II) (0–2 mm/s) and a mixture of Fe(II) and Fe(III) (0–1 mm/s) were evident in the RT spectrum of the day 1 mineral residue from the 0.01-Si-ferrihydrite/1 mmol/L P incubation (Fig. 7a). The spectral area of the Fe(II) doublet (24%) was lower than the extractable Fe(II) concentration of the mineral residue (60–70%, Fig. 3) indicating that Fe(II) also contributed to the central doublet at 0–1 mm/s. The Mössbauer analysis indicated that ~36% of the Fe in the mineral residue was GR, given a GR stoichiometric Fe(II)/Fe(III) ratio of approximately 2 (Drissi et al., 1995). This estimated mass

percent of GR was higher than that qualitatively implied by Figure 5a,ii (<20%), indicating that some GR oxidation occurred during XRD analysis in open air. We term this oxidizable GR compound as GR*. The RT spectrum was modeled with two components: i) Fe(II) from GR and GR* and ii) a combination of Fe(III) from GR and GR* and Fe(II)/Fe(III) from bioaltered ferrihydrite.

Both the Fe(II) and Fe(III) components of the mineral residue were better resolved at 77 K (Fig. 7b). Broadening occurred around the central "doublet" that was now resolved into 3 peaks. The spectra were well described as a combination of i) Fe(II) from GR and GR*, 26%, ii) Fe(III) from GR and GR*, 9%, and iii) bioaltered ferrihydrite containing Fe(II) and Fe(III) that exhibited a broad, collapsed sextet indicative of superparamagnetic behavior [Fe(II)/Fe(III) *spm*], 65%. Zhao et al. (1996) observed superparamagnetically collapsed spectra, similar to our bioaltered *spm* component, for ferrihydrites with sorbed Si at temperatures below 77 K. The *spm* transition temperature was found to be dependent upon the surface coverage of ferrihydrite by Si, and it decreased with an increase in the sorbed Si concentration. The surface speciation of the residual ferrihydrite (if any present) in our bioreduced mineral residue (Figs. 7b,c) is unknown due to significant biomineralization, the presence of bacterial cells and their secretion products, and various chemical components of the media. However, various lines of evidence including the extractable Fe(II) concentration and the Mössbauer behavior of the controls indicated that the *spm* fraction was a mixed Fe(II)/Fe(III) phase and not ferrihydrite with sorbed Si.

The δ value of the *spm* component (0.83 mm/s, Table 1) was consistent with a mixed Fe(II)/Fe(III) phase containing considerable Fe(II). The calculated Fe(II)/Fe(III) ratio of the *spm* phase was 1.3 (from Fig. 7b and chemical extraction). Goya et al. (2003) recently reported a δ value of 0.2 mm/s (derived by QSD method) for a small particle magnetite with a Fe(II)/Fe(III) ratio of ~0.5.

The fraction of GR in the mineral residue increased with incubation time and was the sole product in the 15 month sample (Figs. 7c,d). GR formation was mainly at the expense of the Fe(II)/Fe(III) *spm* phase (also GR*), since the extent of bioreduction (e.g., extractable Fe(II)) did not increase significantly beyond day 1 (Fig. 3). Subtle changes in the *spm* fraction with incubation time and its apparent conversion were evident from the δ values (Table 1) and HFD distributions (Figs. 5b,c inserts). The Fe(II)/Fe(III) ratio of the mineral residue after 15 months of incubation was 2.3 which was in qualitative agreement with stoichiometric GR as reported by Drissi et al. (1995).

3.4.2. The 0.01-Si-ferrihydrite with 4 mmol/L P

The presence of sorbed Fe(II) in the day 1 mineral residue was evident from the increase in the spectral area of Fe(II) that occurred when measurement temperature was decreased from RT to 77 K (24 to 47%, Figs. 8a,b). Such behavior was not observed for the day 1, 1 mmol/L P samples (Fig. 7). Sorbed Fe(II) was distinguished from GR* solely by their different Mössbauer response at RT. Both appeared to oxidize during XRD analysis in open air or were noncrystalline (Fig. 5a-iii). Sorbed Fe(II) was physiochemically undefined and was present in concentration (~23% of Fe) well above what could be expected for an adsorption complex on residual ferrihydrite. The *spm* phase that was prominent in the mineral residue from the 1 and 8 d incubations with 1 mmol/L P was not evident in the Mössbauer spectrum (77 K) of the mineral residue from the 1 d, 4 mmol/L P incubation. Apparently, higher P concentrations blocked its formation. The central doublet (RT and 77 K) was due to residual ferrihydrite and GR* (53%). This assignment was in agreement with the extractable Fe(III) concentration in the mineral residue (~50%; Fig. 3).

The Mössbauer spectra (77 K) of the day 1 and day 8 mineral residues were different from each other, as were their XRD patterns (Figs. 5a,b-iii). In agreement with XRD where GR and vivianite were observed, the 8 d Mössbauer spectrum exhibited a doublet structure consistent with the presence of these phases as primary components. The GR Fe(III) was not explicitly included in the spectral modeling because of ambiguity in the concentration of residual ferrihydrite. However, the XRD analysis implied that its concentration was small (Fig. 5b-iii). Under the assumption that the central doublet resulted from GR, the computed Fe(II)/Fe(III) ratio of the layered hydroxide (1.3) was significantly lower than that produced with 1 mmol/L P (~2, Fig. 7d).

The Mössbauer data in Figure 8 and the stable Fe(II) concentration between days 1 and 8 of incubation (Fig. 3) implied that sorbed Fe(II), GR*, and residual ferrihydrite together transformed into the GR and vivianite with time without significant additional reduction. The transformation of GR* and sorbed Fe(II) to GR was apparent from their Fe(II) QSD distributions (Fig. 8d). A good model fit to the day 1 Mössbauer spectrum could only be obtained using a two-component distribution for the Fe(II) doublet [GR* and sorbed Fe(II)]. A two-component distribution implied significant variation in Fe environments (Rancourt et al., 2001). A narrower QSD distribution for GR Fe(II) in the 8 d sample implied a more defined Fe(II) structural environment.

3.4.3. The 0.01-Si-ferrihydrite with 10 and 20 mmol/L P

The 77 K Mössbauer spectra of the mineral residues from 10 and 20 mmol/L P incubations were dominated by doublets due to GR, vivianite, and residual ferrihydrite (Fig. 9). The mass percent of Fe(II) associated with GR in the 10 mmol/L P sample (Fig. 9a) was similar to the 8 d, 4 mmol/L P sample (Fig. 8c). In contrast, the amount of Fe(II) associated with GR was small [~7% Fe(II)] in the 20 mmol/L P sample (Fig. 9b), where XRD indicated that vivianite was primary crystalline product. The Fe(II)/Fe(III) ratio of GR in the mineral residues from both the 10 and 20 mmol/L P incubations was approximately 1. Most of the central Fe(III) doublet resulted from GR Fe(III) since XRD peaks due to ferrihydrite were not apparent (Figs. 5b-iv,v).

3.4.4. 0.05-Si-ferrihydrite with 1 and 4 mmol/L P

Only limited Mössbauer measurements were performed on mineral residues from the 0.05-Si-ferrihydrite incubations. Analyses were performed on the day 1, 1 and 4 mmol/L P systems where biotransformation to secondary phases was lower than under other conditions.

The Mössbauer spectra (RT and 77 K) of the residues from

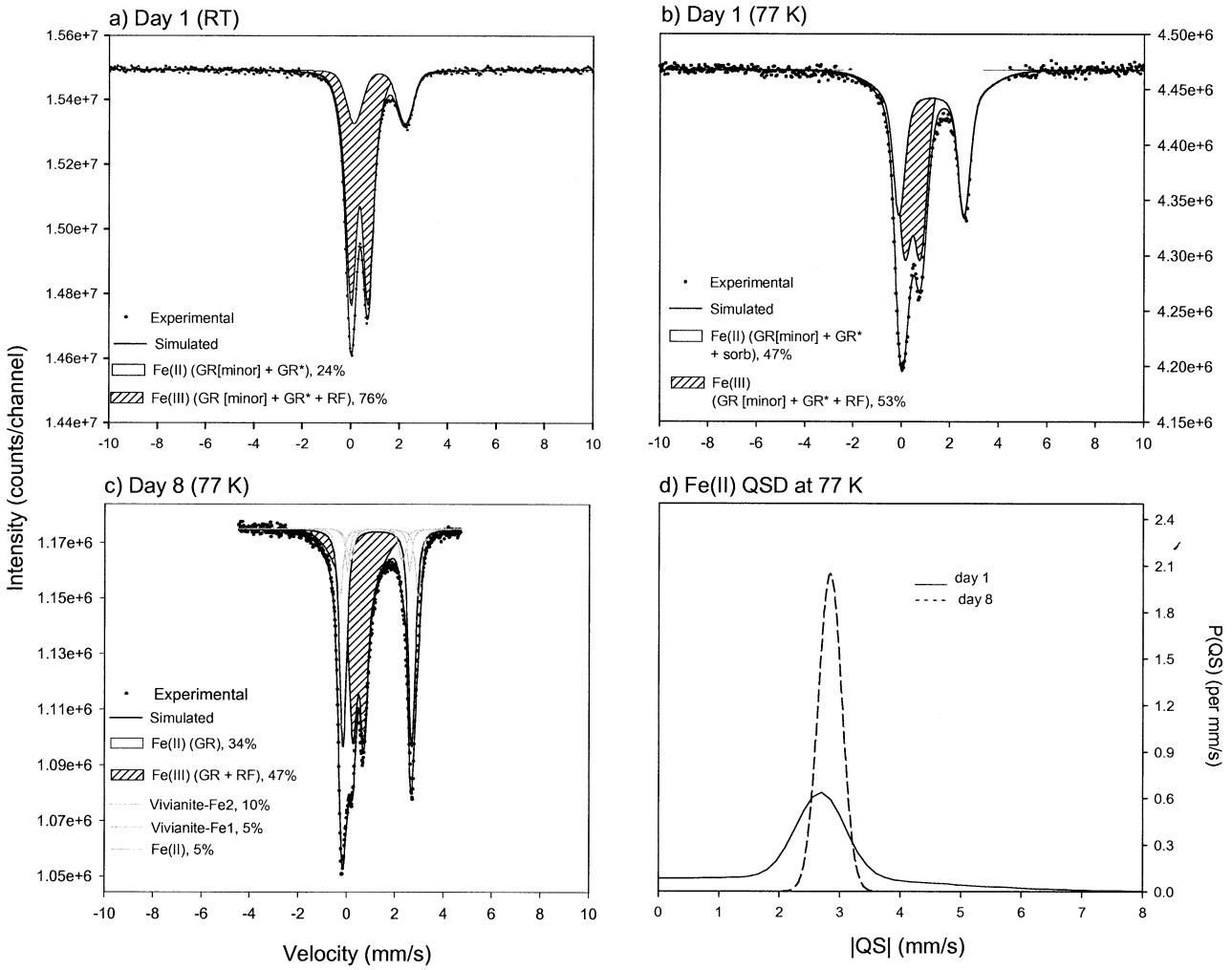

Fig. 8. Mössbauer spectra of 0.01-Si-ferrihydrite/4 mmol/L P after 1 and 8 d incubation. (a, b) RT and 77 K Mössbauer spectra of the day 1 mineral residue. (c) The 77 K Mössbauer spectrum of the 8 d mineral residue and (d) QSD Fe(II) distributions of the day 1 and day 8 samples. RF is residual ferrihydrite. The Fe(II) component not ascribed to either GR or vivianite may be siderite (5% spectral area).

1 mmol/L P, 0.05-Si-ferrihydrite incubations (Figs. 10a,b) differed significantly from those of their 0.01-Si-ferrihydrite counterparts, despite similar XRD patterns (Fig. 5a,iii and 5c,i). Absent was the *spm* phase [mixed Fe(II)/Fe(III) bioaltered ferrihydrite] that dominated the 77 K spectrum of the 0.01-Si-ferrihydrite (Fig. 7b). The Fe(II) doublet contribution to the spectra was similar at RT and 77 K (~45%) which implied the absence of sorbed Fe(II). The spectral area of the Fe(II) doublets, which were a mix of GR (evident from XRD; Fig. 5c-i; <20%) and GR*, was similar to that of the extractable Fe(II) concentration of the mineral residue (Fig. 3, ~45%).

The Mössbauer spectra of the mineral residue from the 4 mmol/L P incubation of 0.05-Si-ferrihydrite (RT and 77 K; Figs. 10c,d), on the other hand, were similar to those of 0.01-Si-ferrihydrite. The presence of sorbed Fe(II) was again apparent from the increase in the spectral area of the Fe(II) doublet on cooling (22 to 41%). Surprisingly, the spectral areas of sorbed Fe(II) (e.g., 19%) and those ascribed to GR* and Fe(III) were quite similar to those of 0.01-Si-ferrihydrite. The spectral area of the Fe(II) doublet was also similar to the extractable Fe(II) concentration of the mineral residue which implied that the central doublet was due to residual ferrihydrite without any *spm* contribution.

3.5. Electron Microscopy

Green rust was visually evident in all samples where XRD and Mössbauer indicated its presence. Hexagonal crystals, characteristic of GR (McGill et al., 1976) were observed to be intermixed with ferrihydrite (Fig. 11; shown for the 0.01-Si-ferrihydrite/1 mmol/L P/d 28 sample as an example). The GR crystallites were ~0.4 to 0.5 μm wide and 0.2 to 0.3 μm thick. Energy dispersive spectroscopy analysis (EDS) showed no evidence for either Cl^- or P in the GR crystallites, providing further evidence for the presence of GR(CO_3^{2-}).

4. DISCUSSION

4.1. Effect of Si

Given the reported inhibitory effect of Si on ferrihydrite crystallization (Cornell et al., 1987; Cornell and Giovanoli,

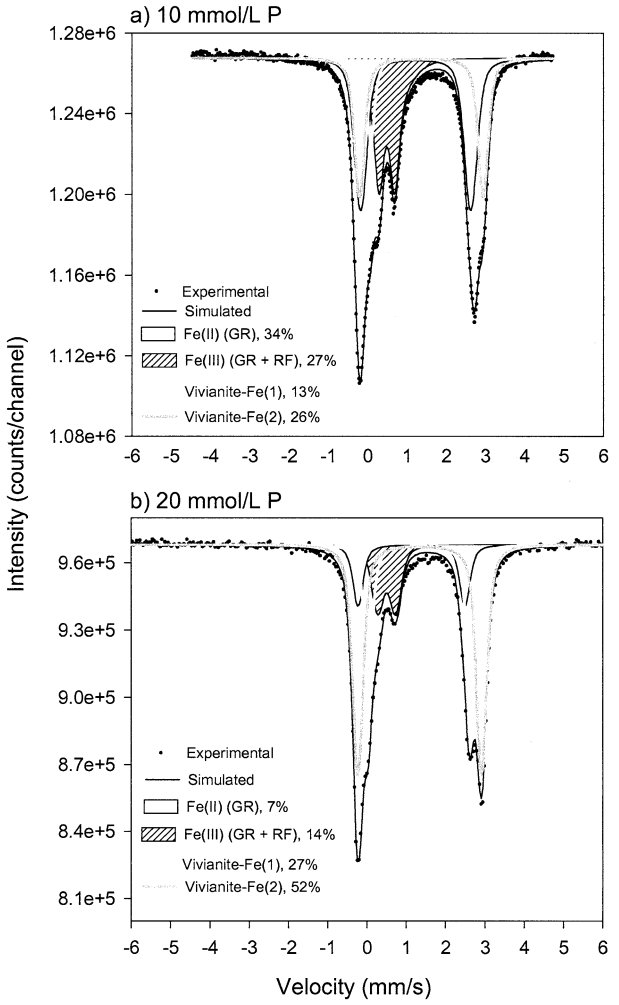

Fig. 9. The 77 K Mössbauer spectra of 0.01-Si-ferrihydrite incubated with CN32 for 8 d with (a) 10 mmol/L P and (b) 20 mmol/L P.

1987), a strong effect of sorbed Si on the rate and extent of ferrihydrite transformation was anticipated under Fe(III)-reducing conditions. However, the common behavior of the 1 and 5 mole % Si coprecipitates noted here (Fig. 3) indicated that Si content (at least in the range studied here) had a small effect on the biotransformation of ferrihydrite in terms of rate, extent, and biomineralization.

Sorbed Si exists as a surface complex [-Fe-O-Si$(OH)_3$] on ferrihydrite at lower Si/Fe ratios (<0.05) and as a structural constituent (-Fe-O-Si- bonds) when Si/Fe >0.10 (Vempati et al., 1990). Ferrihydrite exhibits a higher affinity for phosphate than silicate [as -Fe-O-Si$(OH)_3$]; and PO_4^{3-} displaces $H_3SiO_4^-$ easily from ferrihydrite surfaces (Parfitt, 1978; Vempati and Loeppert, 1989; Parfitt et al., 1992). Since the dissolved Si concentration in the 0.01-Si-ferrihydrite/20 mmol/L P control sample represented 80% of the total Si of the coprecipitate, it appeared that Si was present in the coprecipitate as a loosely bound surface complex. The lower percentages of dissolved Si concentration in the 0.05- vs. the 0.01-Si-ferrihydrite suspensions were not easily explained, but could result from a higher state of Si-polymerization on that surface (Vempati and Loeppert, 1989).

The dissolved Si concentrations of the Si-ferrihydrites incubated with CN32 were significantly lower than the controls (Figs. 1c,d), particularly in the 0.05-Si-ferrihydrite system. Implied was the adsorption of Si by, or coprecipitation within the biogenic secondary solids (magnetite, GR and vivianite). The similar aqueous Si concentration in the day 1 and day 8 samples of the 1 and 4 mmol/L P incubations (in both the Si-ferrihydrites) was intriguing in that day 1 samples were dominated by an apparent Fe(II)/Fe(III) *spm* phase in the 1 mmol/L P 0.01-Si-ferrihydrite incubation, or residual ferrihydrite in the others, whereas all the day 8 samples contained significant GR(CO_3^{2-}) (Fig. 5). Unfortunately, there are no literature accounts of Si adsorption by, or coprecipitation with GR or magnetite to substantiate our hypothesis. The absence of greenalite [$Fe_3Si_2O_5(OH)_4$] and the decrease in aqueous Si concentration between day 1 and day 8 (Fig. 1d) provided additional circumstantial evidence for Si sorption by biogenic products.

Based on a comparison with our previous studies of ferrihydrite biotransformation (Fredrickson et al., 1998, 2001, 2003; Zachara et al., 2002), we believe that Si (with and without P) may have stimulated the rates and extent of ferrihydrite reduction. The rapid conversion of Si-ferrihydrite to magnetite, green rust, and vivianite by CN32 within 1 d (Figs. 5a,c) was quite remarkable. At this point, we do not believe that microbiological factors such as variation in the intrinsic respiration rate of the culture were involved. With pure ferrihydrite in an identical medium, for example, approximately 10% of the total Fe was reduced by CN32 within a day as compared to 50 to 60% in the present study. The effect of Si, however, was less pronounced in the presence of P. The apparent increased bioreducibility of Si-ferrihydrites markedly contrasts with the inhibitory effect of Si on ferrihydrite crystallization to goethite and hematite. Apparently, it is not possible to generalize on the effects of coprecipitated anions on ferrihydrite bioreducibility and mineral transformation. The crystallinity of ferrihydrite may have some effect on bioreduction; ferrihydrites exhibit a continuum in structure from amorphous to partly crystalline (Cornell and Schwertmann, 1996) and aged ferrihydrites demonstrate increased crystallinity and progress toward goethite and hematite. Evidently, sorbed Si makes ferrihydrite more bioavailable to CN32 and more susceptible to mineral transformation by blocking internal condensation reactions involved in ferrihydrite biomineralization (Zachara et al., 2002).

4.2. Biogenic Magnetite

In direct contrast to the effect of P, sorbed Si did not inhibit the formation of magnetite (Fig. 5). However, the RT Mössbauer spectrum of magnetite formed from Si-ferrihydrite was different from that resulting from the bioreduction of metal-substituted (Ni or Co) ferrihydrites, implying an influence of formation rate on biogenic magnetite properties. Magnetite formation in the Si-ferrihydrite system was rapid, occurring within 1–2 d. Its Mössbauer spectrum consisted of a “collapsed” sextet (Fig. 8 of Zachara et al., 2002) characteristic of small particle-size, poorly crystalline magnetite (McNab et al., 1968; Goya et al., 2003). In contrast, bioreduction/biotransformation rates were much slower with Ni and Co-substituted ferrihydrites (Fredrickson et al., 2001; Zachara et al., 2002)

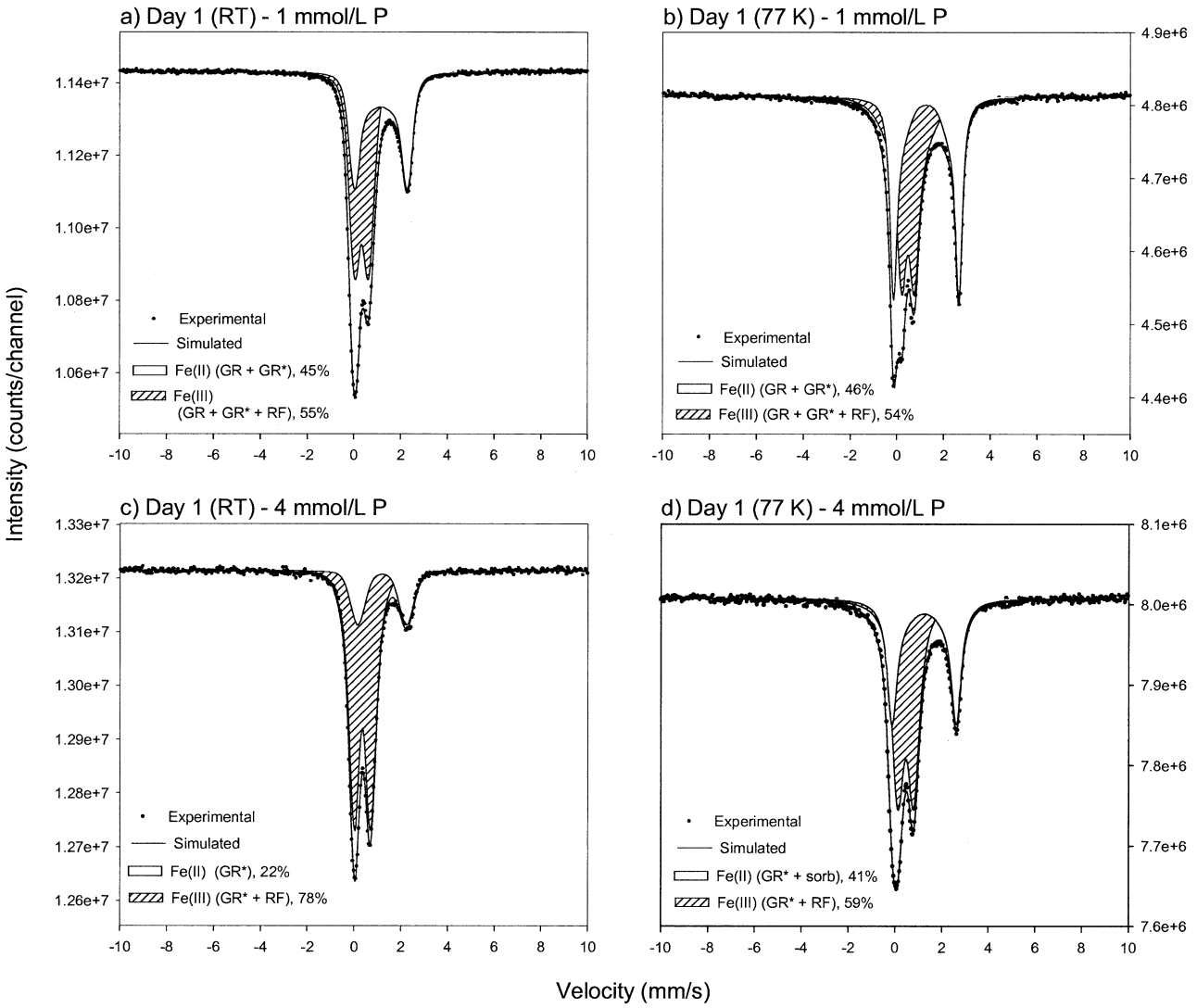

Fig. 10. Mössbauer spectra of 0.05-Si-ferrihydrite mineral residue resulting from incubation with CN32. (a, b) RT and 77 K Mössbauer spectra of day 1, 1 mmol/L P. (c, d) RT and 77 K Mössbauer spectra of day 1, 4 mmol/L P mineral residues.

with 14 to over 30 d required for comparable amounts of magnetite formation. These latter magnetites exhibited RT Mössbauer spectra with well resolved sextets due to octahedral and tetrahedral environments (Fredrickson et al., 2001; Zachara et al., 2002) that were characteristic of well crystalline magnetites (Greenwood and Gibb, 1971). Silica adsorption apparently stabilizes two-line ferrihydrite in a state that allows rapid bioconversion to small particle magnetite.

4.3. Effect of P

Phosphate at any concentration was observed to inhibit magnetite formation. Phosphate appeared to be essential for biogenic GR formation, based on a comparison of media without P (magnetite) and with 1 mmol/L P (GR) (Fig. 5). These two bioreduced ferrihydrite suspensions contained similar concentrations of 0.5 N HCl extractable and aqueous Fe(II) (Fig. 3). At higher P concentrations, as noted with pure ferrihydrite (Fredrickson et al., 1998), a GR-vivianite mineral association was generated by CN32. Vivianite appears to be a more stable phase than GR in the presence of P (Hansen and Poulsen, 1999), and, under the chemical conditions of our experiments, exhibits more rapid precipitation kinetics than GR. The GR to vivianite ratio in our experiments was controlled primarily by the total P concentration. Given the stochiometry of vivianite [$Fe_3(PO_4)_2 \cdot 8H_2O$], our total P concentrations (4, 10, and 20 mmol/L) would support the precipitation of 12, 30, and 60% of the total Fe as vivianite, if the Fe was present as Fe(II). Our modeling of the Mössbauer spectral areas (e.g., Figs. 8 and 9) suggested the presence of vivianite at mass concentrations of 15, 39, and 79%. These were higher than, but in qualitative agreement with expectation. The role of P on promoting GR formation, however, was not clear. Phosphate may promote GR formation by kinetically inhibiting the transformation to more stable magnetite.

Strong surface complexation of P with ferrihydrite apparently prevents the solid-state transformation of ferrihydrite to

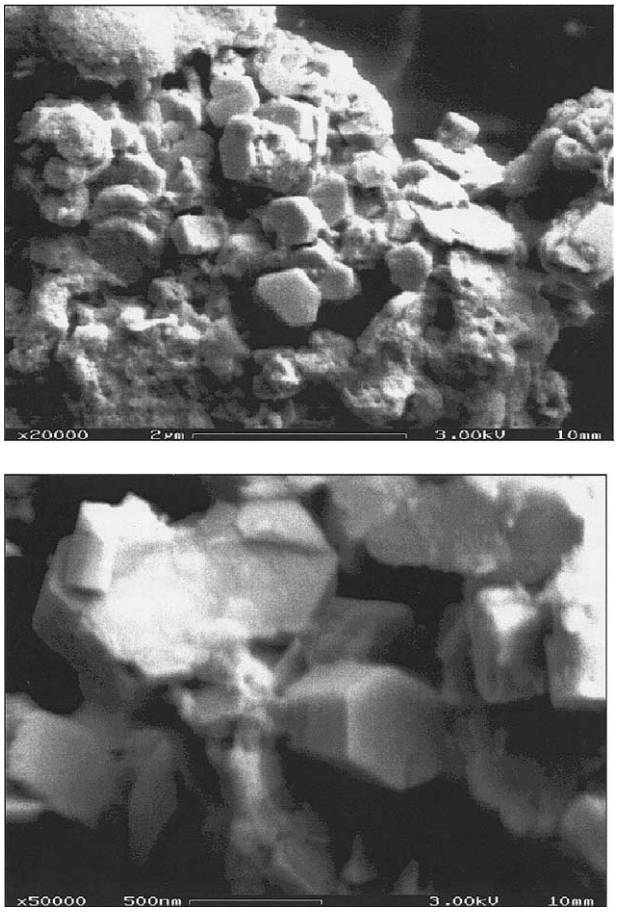

Fig. 11. Scanning electron micrographs of 0.01-Si-ferrihydrite incubated with CN32 and 1 mmol/L P for 28 d, showing the presence of 0.4 to 0.5 μm hexagonal GR crystals mixed with residual ferrihydrite.

magnetite (Couling and Mann, 1985). The adsorption densities and aqueous concentration range over which P inhibits magnetite formation have not been established in either abiotic or biotic systems. It appears, however, that surface saturation is not essential for magnetite inhibition since GR(CO_3^{2-}) was observed as the primary biotransformation product in the 1 mmol/L P media with both the Si-ferrihydrites. An aqueous concentration of 1 mmol/L P yields an adsorption density of 0.21 mmol of P/g of ferrihydrite, which is significantly lower than the reported absorption maxima (2 mmol of P/g). Increased vivianite formation was observed at P concentrations that exceeded surface saturation (e.g., 10 mmol/L P). Vivianite has a lower solubility (Al-Borno and Tomson, 1994) than either GR (Génin et al., 1998) or siderite (Bruno et al., 1992), and forms rapidly under circumneutral conditions (Fredrickson et al., 1998).

4.4. Biogenic Green Rust

4.4.1. GR composition and Fe(II)/Fe(III) ratio

The aqueous concentration of Cl^- and inorganic C, and the EDS analysis of hexagonal precipitates for P and Cl^- allowed us to conclude that the biogenic GR was intercalated with carbonate [GR(CO_3^{2-})]. The absence of GR(Cl^-) was surprising because the medium contained 28 mmol/L Cl^-. Similarly, Abdelmoula et al. (1996) observed the formation of GR(CO_3^{2-}) in a bicarbonate/chloride solution containing excess Cl^- (Cl^-:HCO_3^- ~40:1). X-ray diffraction conclusively showed that GR(PO_4^{3-}) did not form in our experiments, in spite of the presence of P in the media. In contrast, Parmar et al. (2001) reported the biosynthesis of GR(PO_4^{3-}) from Ni-ferrihydrite by CN32. Our finding of GR(CO_3^{2-}) implied that GR has a higher affinity for CO_3^{2-} than either Cl^- or P. Hydrotalcites show a strong preference for CO_3^{2-} over SO_4^{2-} and PO_4^{3-}(Miyata et al., 1975), presumably for reasons of charge density.

The Fe(II)/Fe(III) ratio of the biogenic GR(CO_3^{2-}) varied with the P concentration. Both stochiometric (2:1; Drissi et al., 1995) and nonstochiometric GRs were formed. Green rusts with a variable Fe(II)/Fe(III) ratio were recently reported by Ona-Nguema et al. (2002). In the present study, GRs with an Fe(II)/Fe(III) ratio of approximately 2 were formed when the P concentration was <1 mmol/L (Fig. 7d), whereas GRs with an Fe(II)/Fe(III) ratio of approximately 1.3 were formed at higher P concentrations (Figs. 8c and 9). The differences in the Fe(II)/Fe(III) ratio between the variable P samples were clearly evident in a comparison of the 15 month, 1 mmol/L P sample (Fig. 7d) and the 8 d, 10 mmol/L P bioreduced sample (Figs. 8c and 9a). The noted variations in the Fe(II)/Fe(III) ratio suggested that the P adsorption density, rather than the rates and extent of bioreduction of ferrihydrite, dictated the Fe(II)/Fe(III) ratio in the GR product.

4.4.2. Formation pathways

Two primary routes of GR formation were observed that varied with Si and P concentration. In the medium with the lowest Si and P concentrations (1 mole % Si and 1 mmol/L P), we observed the formation of bioaltered ferrihydrite with superparamagnetic behavior (the *spm* phase) after 1 d of incubation. This phase transformed (along with minor GR*) to a stochiometric GR during 15 months of incubation. The *spm* phase contained Fe(II) and Fe(III) (Figs. 3 and 7 and Table 1 [δ-value]) with Fe(II) in structural sites. It was clearly differentiated from ferrihydrite with adsorbed Si and P (1 mmol/L P control sample; Fig. 6a) by 77 K Mössbauer spectroscopy. Green rust was found in association with the *spm* phase after only 1 d of incubation, suggesting either a common or a competitive formation mechanism. Perhaps one of these phases formed in close proximity to the bacterial surface where the pH, Fe(II) and CO_3^{2-}/acetate flux were higher. Why this *spm* phase evolved to GR as opposed to more stable magnetite was not evident, but P exerted a pivotal role. The formation of the *spm* phase was inhibited by higher P and Si concentrations.

The second synthesis route was observed at higher P concentrations (1 mole % Si and 4 mmol/L P). Green rust*, sorbed Fe(II), and residual ferrihydrite that were evident after 1 d of incubation transformed to GR over an approximate 7 d period (Fig. 8). Mössbauer measurements of the day one sample (Figs. 8a,b) showed that GR* Fe(II) and sorbed Fe(II) were in nondistinct environments that were structurally different from the *spm* phase observed with 1 mmol/L P. Perhaps the state of sorbed Fe(II) in this residue was akin to a poorly crystalline $Fe(OH)_2$ coprecipiate or surface precipitate (Pecher et al.,

2000) associated with ferrihydrite. The Mössbauer parameters of sorbed Fe(II) were significantly different from those reported for $Fe(OH)_2$ (Koch, 1998). We speculate that this same mechanism of GR formation was operative at 10 mmol/L P (Figs. 5a and 5b-iv), and for the 0.05-Si-ferrihydrite coprecipitate (Fig. 5c) where GR concentrations increased markedly between 1 and 8 d. While the diffraction analyses of the 0.01-Si-ferrihydrite sample incubated with 10 mmol/L P for 1 and 8 d could imply GR formation at the expense of vivianite, this was not the case as the vivianite concentration after 1 d had reached the maximum allowable by the total P concentration (e.g., 15 mmol/L of Fe or 30% of Fe_{total}). Consequently, the GR that formed between day 1 and day 8 was believed to result from the transformation of ferrihydrite with sorbed Fe^{2+} like that in shown in Figure 8a.

Unresolved for both these formation paths was whether GR was mediated by bacterial action or was the result of abiotic crystallization kinetics under the specific chemical regimes. Generally, the Fe(II)/Fe(III) ratio did not change during the time periods of GR formation, thus arguing against bacterial involvement. GR formation is believed to occur via solid-state rearrangement of ferrihydrite promoted by Fe^{2+} adsorption (Mann et al., 1989; Hansen et al., 1994; Fredrickson et al., 1998), although little direct evidence exists for this mechanism. The detection of GR* Fe(II), sorbed Fe(II), structural Fe(II) (*spm*), and the complete conversion of these phases to crystalline GR lends further support to a solid-state transformation mechanism. However, the large size of the GR crystals (Fig. 11) was difficult to rationalize as a consequence of solid-state transformation of $<$10 nm ferrihydrite particles unless significant particle aggregation occurred during crystal growth.

4.5. Environmental Implications

We have observed that the biotransformation of two-line ferrihydrite to GR in the laboratory is sensitive to P concentration, but not to Si. Our experiments contained high organism concentrations (10^8 cells/mL), excess electron donor (lactate), and AQDS (an electron shuttle). These three factors enhanced the bioreduction rate of Fe(III) by CN32. In-situ bioreduction rates in groundwater or sediment are likely to be much slower for various reasons including organism density and electron donor concentrations, and yield different mineralogic products. We have previously shown (Zachara et al., 2002) that the nature of mineral products resulting from the biotransformation of ferrihydrite are a complex function of many variables including electron acceptor to donor ratios and other factors controlling Fe(II) production rate. Whether our findings regarding GR biosynthesis and the pathways involved are relevant to subsurface environments or are artifacts of the specific experimental conditions remains to be seen. Experiments under relevant in-situ conditions, whatever they may be, are a clear need.

AQDS was used as a media component in low concentration because previous studies by our laboratory have shown that it was necessary to produce crystalline GR (Fredrickson et al., 1998). The mechanistic role of AQDS in GR synthesis is not known but is currently under investigation by our laboratory. Others, however, have, observed biogenic GR synthesis without AQDS (Parmar et al., 2001; Ona-Nguema et al., 2002), so perhaps its presence is not essential. AQDS has been used by some as an analog of the quinone component of dissolved natural organic matter (DOM; Lovley et al., 1996; Lovley et al., 1998; Nevin and Lovley, 2000; Klapper et al., 2002), leaving open the question as to whether DOM may promote environmental GR formation.

Some have suggested that Fe(II)-hydroxide and GRs adsorb P in anoxic soils and sediments (Williams et al., 1971; Patrick and Khalid, 1974; Willett and Higgins, 1978, Holford and Patrick, 1979). However, our results are not necessarily supportive of that point. Hansen and Poulsen (1999) studied P adsorption by synthetic GR(SO_4^{2-}) and concluded that, while P may exchange as an interlayer anion, GR(PO_4^{3-}) is metastable and transforms to vivianite, the stable end product. In the present study, we have observed the precipitation of GR-vivianite mixtures without any evidence for the intermediate formation of GR(PO_4^{3-}). These results imply that GR(CO_3^{2-}) has low affinity for P and that this phase is unlikely to function as an important sorbent for P in anoxic soils.

Mössbauer analyses indicated that the biogenic GR's formed in our experiments exhibited variable Fe(II)/Fe(III) ratios (between 1 and 2). Increasing P lead to a decrease in Fe(II)/Fe(III) ratio for unexplained reasons. Green rusts are contaminant reductants (Hansen et al., 1996; Myneni et al., 1997; Erbs et al., 1999; Lee et al., 2000; Loyaux-Lawniczak et al., 2000; Refait et al., 2000; Williams and Scherer, 2001; Bond and Fendorf, 2003), and sorbents for divalent cations such as Ni^{2+}, Co^{2+}, and Zn^{2+} that may substitute for structural Fe(II) (Refait and Génin, 1997; Génin et al., 1998; Parmar et al., 2001). Our results indicate that the influence of Fe(II)/Fe(III) ratio on these processes should be considered because GR's with variable ratios may form in anoxic environments through bacterial activity. The Fe(II)/Fe(III) ratio may effect the redox chemistry, solubility, and ion exchange properties of the GR (Refait and Génin 1997; Génin et al., 1998; Parmar et al., 2001).

Karim (1986) studied the effect of Si on the neutralization and oxidation of acidic ferrous chloride solutions. Lepidocrocite and ferrihydrite were generated in absence and presence of Si, respectively, via GR-like intermediate structures. A "more" crystalline GR intermediate was formed in absence of Si. Apparently Si prevented GR transformation to lepidocrocite, probably due to structural considerations. The presence of adsorbed or coprecipitated Si within our biogenic GRs, as implied by the aqueous phase analysis in Figure 1, therefore, may affect its reaction with molecular oxygen or other contaminant oxidants such CrO_4^{2-}, SeO_4^{-} or UO_2^{2+}. Additional research is needed to evaluate this issue.

Acknowledgments—This research was sponsored by the Chemical Sciences Division (Geosciences Program), Basic Energy Sciences (BES), U.S. Department of Energy (DOE). Mössbauer, X-ray diffraction, and electron microscopic analyses were performed at the W. R. Wiley Environmental and Molecular Sciences Laboratory, a national scientific user facility sponsored by the U. S. Department of Energy's Office of Biological and Environmental Research and located at the Pacific Northwest National Laboratory. PNNL is operated for the Department of Energy by Battelle. We also would like to thank Steven C. Smith, Colleen K. Russell, Tom W. Wietsma, and Alice C. Dohnalkova of PNNL for their help with the Si-ferrihydrite synthesis; XRD and

Mössbauer analyses; ICP, Cl-, and inorganic C analyses; and electron microscopy.

Associate editor: D. J. Vaughan

REFERENCES

Abdelmoula M., Refait P., Drissi S. H., Mihe J. P., and Génin J.-M. R. (1996) Conversion electron Mössbauer spectroscopy and X-ray diffraction studies of the formation of carbonate-containing green rust one by corrosion of metallic iron in $NaHCO_3$ and ($NaHCO_3$ + NaCl) solutions. *Corr. Sci.* **38,** 623–633.

Al-Borno A. and Tomson M. B. (1994) The temperature dependence of the solubility product constant of vivianite. *Geochim. Cosmochim. Acta* **58,** 5373–5378.

Bernal J. D., Dasgupta D. T., and Mackay A. L. (1959) The oxides and hydroxides of iron and their structural inter-relationships. *Clay Mineral. Bull.* **4,** 15–30.

Bond L. D. and Fendorf S. (2003) Kinetics and structural constraints of chromate reduction by green rust. *Environ. Sci. Technol.* **37,** 2750–2757.

Bruno J., Wersin P., and Stumm W. (1992) On the influence of carbonate in mineral dissolution: II. The solubility of $FeCO_3$(s) at 25°C and 1 atm total pressure. *Geochim. Cosmochim. Acta* **56,** 1149–1155.

Carlson L. and Schwertmann U. (1981) Natural ferrihydrites in surface deposits from Finland and their association with silica. *Geochim. Cosmochim. Acta* **45,** 421–429.

Cornell R. M. and Giovanoli R. (1987) The influence of silicate species on the morphology of goethite (α-FeOOH) grown from ferrihydrite ($5Fe_2O_3 \cdot 9H_2O$). *JCS Chem. Commun.* 413–414.

Cornell R. M., Giovanoli R., and Schindler P. W. (1987) Effect of silicate species on the transformation of ferrihydrite into goethite and hematite in alkaline media. *Clays Clay Miner.* **35,** 21–28.

Cornell R. and Schwertmann U. (1996) The Iron Oxides: Structure, Properties, Reactions, Occurrences and Use. VCH.

Couling S. B. and Mann S. (1985) The influence of inorganic phosphate on the crystallization of magnetite (Fe_3O_4) from aqueous solution. *JCS Chem. Comm.* 1713–1715.

Diamant A. and Pasternak M. (1982) Characterization of adsorbed iron in montmorillonite by Mössbauer spectroscopy. *Clays Clay Miner.* **30,** 63–66.

Drissi H., Refait P., Abdelmoula M., and Génin J.-M. R. (1995) The preparation and thermodynamic properties of Fe(II)-Fe(III) hydroxycarbonate (green rust one): Pourbaix diagram of iron in carbonate-containing aqueous media. *Corros. Sci.* **37,** 2025–2041.

Erbs M., Hansen H. C. B., and Olsen C. E. (1999) Reductive dechlorination of carbon tetrachloride using iron(II) iron(III) hydroxide sulfate (green rust). *Environ. Sci. Technol.* **33,** 307–311.

Fortin D., Leppard G. G., and Tessier A. (1993) Characteristics of lacustrine diagenetic iron oxyhydroxides. *Geochim. Cosmochim Acta* **57,** 4391–4404.

Fox L. E. (1989) The solubility of colloidal ferric hydroxide and its relevance to iron concentrations in river water. *Geochim. Cosmochim Acta* **52,** 771–777.

Fredrickson J. K., Zachara J. M., Kennedy D. W., Dong H., Onstottt T. C., Hinman N. W., and Li S. (1998) Biogenic Fe mineralization accompanying the dissimilatory reduction of hydrous ferric oxide by a ground water bacterium. *Geochim. Cosmochim. Acta* **62,** 3239–3257.

Fredrickson J. K., Zachara J. M., Kukkadapu R. K., Gorby Y. A., Smith S. C., and Brown C. F. (2001) Biotransformation of Ni-substituted hydrous ferric oxide by an Fe(III)-reducing bacterium. *Environ. Sci. Technol.* **35,** 703–712.

Fredrickson J. K., Kota S., Kukkadapu R. K., Liu C., and Zachara J. M. (2003) Influence of electron donor/acceptor concentrations on hydrous ferric oxide (HFO) bioreduction. *Biodegradation* **14,** 91–203.

Génin J.-M. R., Bourrié G., Trolard F., Abdelmoula M., Jaffrezic A., Refait O., Maitre V., Humbert B., and Herbillion A. (1998) Thermodynamic equilibria in aqueous suspensions of synthetic and natural Fe(II)-Fe(III) green rusts: Occurrences of the mineral in hydromorphic soils. *Environ. Sci. Technol.* **32,** 1058–1068.

Gonser U. and Grant R. W. (1967) Determination of spin directions and electric field gradient axes in vivianite by polarized recoil γ-free rays. *Phys. Stat. Sol.* **21,** 331.

Goya G. F., Berquó T. S., and Fonseca C. F. (2003) Static and dynamic magnetic properties of spherical magnetite nanoparticles. *J. Appl. Phys.* **94,** 3520–3528.

Greenwood N. N. and Gibb T. C. (1971) Mössbauer Spectroscopy. Chapman and Hall.

Hansen H. C. B., Borggaard O. K., and Sorensen J. (1994) Evaluation of the free energy of formation of Fe(II)-Fe(III) hydroxide-sulphate (green rust) and it's reduction of nitrite. *Geochim. Cosmochim. Acta* **58,** 2599–2608.

Hansen H. C. B., Koch C. B., Nancke-Krogh H., Borggaard O. K., and Sørensen J. (1996) Abiotic nitrate reduction to ammonium: Key role of green rust. *Environ. Sci. Technol.* **30,** 2053–2056.

Hansen H. C. B. and Poulsen I. F. (1999) Interaction of synthetic sulphate "green rust" with phosphate and the crystallization of vivianite. *Clays Clay Miner.* **47,** 312–318.

Holford I. C. R. and Patrick W. H., Jr.. (1979) Effects of reduction and pH changes on phosphate sorption and mobility in an acid soil. *Soil Sci. Soc. Am. J.* **43,** 292–297.

Kandori K., Uchida S., Kataoka S., and Ishikawa T. (1992) Effects of silicate and phosphate ions on the formation of ferric oxide hydroxide particles. *J. Mater. Sci.* **27,** 719–728.

Karim Z. (1986) Formation of ferrihydrite by inhibition of green rust structures in the presence of silicon. *Soil Sci. Soc. Am. J.* **50,** 247–250.

Klapper L., McKnight D. M., Fulton J. R., Blunt-Harris E. L., Nevin K. P., Lovley D. R., and Hatcher P. G. (2002) Fulvic acid oxidation state detection using fluorescence spectroscopy. *Environ. Sci. Technol.* **36,** 3170–3175.

Koch C. B. (1998) Structures and properties of anionic clay minerals. *Hyperfine Interactions* **117,** 131–157.

Kukkadapu R. K., Zachara J. M., Fredrickson J. K., Smith S. C., Dohnalkova A. C., and Russell C. K. (2003) Transformation of 2-line ferrihydrite to 6-line ferrihydrite under oxic and anoxic conditions. *Am. Miner.* **88,** 1903–1914.

Lee N., Batchelor W., and Schlautman M. A. (2000) Reductive capacity of soil for chromium. *Environ Sci. Technol.* **21,** 953–963.

Lovley D. R. and Phillips E. J. P. (1986) Availability of ferric iron for microbial reduction in bottom sediments of the freshwater tidal Potomac River. *Appl. Environ. Microbiol.* **52,** 751–757.

Lovley D. R., Coates J. D., Blunt-Harris E. L., Phillips E. J. P., and Woodward J. C. (1996) Humic substances as electron acceptors for microbial respiration. *Nature* **382,** 445–448.

Lovley D. R., Fraga J. L., Blunt-Harris E. L., Hayes L. A., Phillips E. J. P., and Coates J. D. (1998) Humic substances as a mediator for microbially catalyzed metal reduction. *Acta Hydrochim. Hydrobiol.* **26,** 152–157.

Loyaux-Lawniczak S., Refait P., Ehrhardt J.-J., Lecomte P., and Génin J.-M. R. (2000) Trapping of. Cr by formation of ferrihydrite during the reduction of chromate ions by Fe(II)-Fe(III) hydoxysalt green rusts. *Environ. Sci. Technol.* **34,** 438–443.

Mann S., Sparks N. H. C., Couling S. B., Larcombe M. C., and Frankel R. B. (1989) Crystallochemical characterization of magnetic spinels prepared from aqueous solution. *JCS Faraday Trans. I* **85,** 3033–3044.

McGill I. R., McEnaney B., and Smith D. C. (1976) Crystal structure of green rust formed by corrosion of cast iron. *Nature* **259,** 200–201.

McNab T. K., Fox R. A., and Boyle A. J. F. (1968) Some magnetic properties of magnetite (Fe_3O_4) microcrystals. *J. Appl. Phys.* **39,** 5703–5711.

Miyata S., Kumura T. and Shimada M. (1975) Composite metal hydroxides. U.S. Patent 3,879,523.

Murad E. and Schwertmann U. (1988) The characterization of poorly crystalline Si-containing natural iron oxides by Mössbauer spectroscopy. *Hyperfine Interactions* **41,** 835–838.

Myneni S. C. B., Tokunaga T. K., and Brown G. E., Jr. (1997) Abiotic selenium redox transformations in the presence of Fe(II, III) oxides. *Science* **278,** 1106–1109.

Nevin K. P. and Lovley D. R. (2000) Potential for nonenzymatic reduction of Fe(III) via electron shuttling in subsurface sediments. *Environ. Sci. Technol.* **34,** 2472–2478.

Ona-Nguema G., Abdelmoula M., Jorand F., Benali O., Géhin A., Block J-C., and Génin J.-M. R. (2002) Iron (II, III) hydroxycarbonate green rust formation and stabilization from lepidocrocite bioreduction. *Environ. Sci. Technol.* **36,** 16–20.

Parfitt R. L. (1978) Anion adsorption by soils and soil materials. *Adv. Agron.* **30,** 1–50.

Parfitt R. L., Gaast S. J. V., and Childs C. W. (1992) A structural model for natural siliceous ferrihydrite. *Clays Clay Miner.* **40,** 675–681.

Parmar N., Gorby Y. A., Beveridge T. J., and Ferris F. G. (2001) Formation of green rust and immobilization of nickel in response to bacterial reduction of hydrous ferric oxide. *Geomicrobiol. J.* **18,** 375–385.

Patrick W. H., Jr. and Khalid R. A. (1974) Phosphate release and sorption by soils and sediments: Effect of aerobic and anaerobic conditions. *Science* **186,** 53–55.

Pecher K., Haderlein S. B., and Schwarzenbach R. P. (2000) Reduction of polyhalogenated methanes by surface-bound Fe(II) in aqueous suspension of iron-oxides. *Environ. Sci. Technol.* **36,** 1734–1741.

Perret D., Gaillard J-F., Dominik J., and Atteia O. (2000) The diversity of hydrous iron oxides. *Environ. Sci. Technol.* **34,** 3540–3546.

Rancourt D. G. and Ping J. Y. (1991) Voigt-based methods for arbitrary-shape static hyperfine parameter distribution in Mössbauer spectroscopy. *Nucl. Instr. Methods Phys. Res. B* **58,** 85–97.

Rancourt D. G., Fortin D., Pichler T., Thibault P-J., Lamarche G., Morris R. V., and Mercier P. H. J. (2001) Mineralogy of a natural As-rich hydrous ferric oxide coprecipitate formed by mixing of hydrothermal fluid and sea water: Implications regarding surface complexation and color banding in ferrihydrite deposits. *Am. Miner.* **86,** 834–851.

Reeves N. J. and Mann S. (1991) Influence of inorganic and organic additives on the tailored synthesis of iron oxides. *JCS Faraday Trans. I* **87,** 3875–3880.

Refait P. and Génin J.-M. R. (1997) Mechanisms of oxidation of Ni(II)-Fe(II) hydroxides in chloride containing aqueous media: Role of the pyroaurite-type Ni-Fe hydroxychlorides. *Clay Miner.* **32,** 597–613.

Refait P., Simon L., and Génin J.-M R. (2000) Reduction of SeO_4^{2-} anions and anoxic formation of iron(II)-iron(III) hydroxy-selenate green rust. *Environ. Sci. Technol.* **34,** 819–825.

Rouzies D. and Millet J. M. M. (1993) Mössbauer study of synthetic oxidized vivianite at room-temperature. *Hyperfine Interactions* **77,** 19–28.

Ryden J. C., McLaughlin J. R., and Syers J. K. (1977) Mechanism of phosphate sorption by soils and hydrous ferric oxide gels. *J. Soil Sci.* **28,** 72–92.

Stookey L. L. (1970) Ferrozine-a new spectrophotometric reagent for iron. *Anal. Chem.* **42,** 779–781.

Taylor H. F. W. (1973) Crystal structures of some double layered hydroxide minerals. *Mineral. Mag.* **39,** 377–389.

Tessier A., Fortin D., Belzile N., DeVitre R. R., and Leppard G. (1996) Metal sorption to diagenetic iron and manganese oxyhydroxides and associated organic matter: Narrowing the gap between field and laboratory measurements. *Geochim. Cosmochim. Acta* **60,** 387–404.

Trolard F., Génin J.-M. R., Abdelmoula M., Bourrié G., Humbert B., and Herbillion A. (1997) Identification of a green rust mineral in reductomorphic soil by Mössbauer and Raman spectroscopies. *Geochim. Cosmochim. Acta* **61,** 1107–1111.

Vempati R. K. and Loeppert R. H. (1989) Influence of structural and adsorbed Si on the transformation of synthetic ferrihydrite. *Clays Clay Miner.* **37,** 273–279.

Vempati R. K., Loeppert R. H., Dufner D. C., and Cocke D. L. (1990) X-ray photoelectron spectroscopy as a tool to differentiate silicon-bonding state in amorphous iron oxides. *Soil Sci. Soc. Am. J.* **54,** 695–698.

Waychunas G. A., Fuller C. C., Rea B. A., and Davis J. A. (1996) Wide angle X-ray scattering (WAXS) study to "two-line" ferrihydrite structure: Effect of arsenate sorption and counter anion variation and comparison with EXAFS results. *Geochim. Cosmochim. Acta* **60,** 1765–1781.

Willett I. R. and Higgins M. L. (1978) Phosphate sorption by reduced and reoxidized rice soils. *Aust. J. Soil Res.* **16,** 319–326.

Williams J. D. H., Syers J. K., Shukla S. S., Harris R. F., and Armstrong D. E. (1971) Levels of inorganic and total phosphate in lake sediments as related to other sediment parameters. *Environ. Sci. Technol.* **5,** 1113–1120.

Williams A. G. B. and Scherer M. M. (2001) Kinetics of Cr(VI) reduction by carbonate green rust. *Environ. Sci. Technol.* **35,** 3488–3494.

Zachara J. M., Fredrickson J. K., Li S. W., Kennedy D. W., Smith S. C., and Gassman P. L. (1998) Bacterial reduction of crystalline Fe(III) oxides in single phase suspensions and subsurface materials. *Am. Mineral.* **83,** 1426–1443.

Zachara J. M., Kukkadapu R. K., Fredrickson J. K., Gorby Y. A., and Smith S. C. (2002) Biomineralization of poorly crystalline Fe(III) oxides by dissimilatory metal reducing bacteria (DMRB). *Geomicrobiol. J.* **19,** 179–207.

Zhao J., Huggins F. E., Feng Z., and Huffman G. P. (1994) Ferrihydrite: Surface structure and its effects on phase transformation. *Clays Clay Miner.* **42,** 737–746.

Zhao J., Huggins F. E., Feng Z., and Huffman G. P. (1996) Surface-induced superparamagnetic relaxation in nanoscale ferrihydrite particle. *Phys. Rev. B* **54,** 3403–3407.